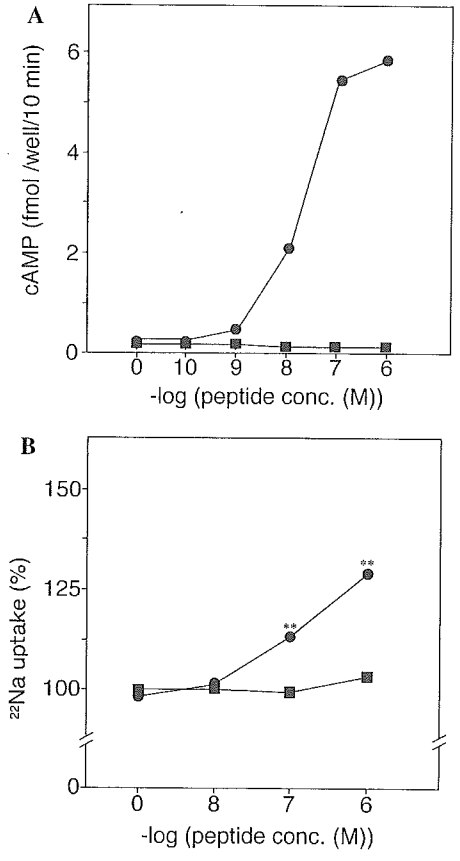

Fig. 4. Effects of CRSP-1 on the intracellular cAMP level (A) and the $^{22}Na^{+}$ uptake (B) into intact OK cells and OK cells transfected with porcine CT receptor. (A) OK cells transfected with porcine CT receptor cDNA (closed circle) and blank vector (closed square) were stimulated with the indicated concentrations of CRSP-1 for 10 min. (B) OK cells transfected with porcine CT receptor cDNA (closed circle) and blank vector (closed square) were incubated with $^{22}Na^{+}$ and the indicated concentrations of CRSP-1 for 10 min. Each point represents the mean ± SEM of three separate determinations. $^{**}P < 0.001$.

effect of CRSP-1 on the $^{22}Na^{+}$ uptake into LLC-PK$_1$ cells (Fig. 5C). These results indicate that the CRSP-1-induced enhancement of $^{22}Na^{+}$ uptake is mediated by a Na^{+}/H^{+} exchanger (NHE).

To identify which isoform of NHEs is responsible for the $^{22}Na^{+}$ uptake that is enhanced by CRSP-1, we treated the cells with different concentrations of EIPA from 1×10^{-8} to 1×10^{-6} M (Fig. 6). The inhibitory effect of EIPA was observed even at a concentration of 1×10^{-8} M. When CRSP-1 and EIPA were administered together at concentrations of 1×10^{-6} M, the effect of CRSP-1 on the $^{22}Na^{+}$ uptake into LLC-PK$_1$ cells was abolished, and the $^{22}Na^{+}$ uptake was reduced to that level when only EIPA had been added to the medium.

Discussion

The effects of CT on renal epithelial cells are known to be mediated by the CT receptor-cAMP pathway [4]. In preceding studies, we demonstrated that porcine CRSP-1 is a more potent and specific agonist for the CT receptor. In the present study, therefore, we investigated the effect of CRSP-1 on the cell physiological events that were induced by the elevation of the cAMP production in the renal epithelial cell line, LLC-PK$_1$.

Fig. 1 shows the anti-proliferative effect of CRSP-1, as well as its stimulatory effect on cAMP production in LLC-PK$_1$ cells, and these effects were 10-fold stronger than those of porcine CT. CT inhibits the growth of LLC-PK$_1$ cells by increasing the intracellular cAMP concentration [6,7]. Jans et al. [6] reported that the growth of LLC-PK$_1$ cells having a mutation in the cAMP-dependent protein kinase (A-kinase) was not inhibited with salmon CT or a vasopressin analogue. Taking these results together, CRSP-1 was deduced to suppress the proliferation of LLC-PK$_1$ through the cAMP-A-kinase pathway.

CRSP-1 and salmon CT reduced $^{45}Ca^{2+}$ uptake into the LLC-PK$_1$ cells (Fig. 2). Several in vivo studies have revealed that urinary Ca^{2+} reabsorption is regulated by the balance between the passive Ca^{2+} influx across the apical membrane via an electrochemical gradient and the active Ca^{2+} extrusion across the basolateral membrane induced with Ca^{2+} pumps and Na^{+}/Ca^{2+} exchangers [8]. Although we cannot specify the target of the CRSP-1-induced suppression of Ca^{2+} uptake, this result raises the possibility that CRSP-1 reduces the plasma Ca^{2+} concentration by inhibiting urinary Ca^{2+} reabsorption into the renal epithelial cells in the kidney.

The $^{22}Na^{+}$ uptake into LLC-PK$_1$ cells was enhanced with CRSP-1 (Fig. 3A). The $^{22}Na^{+}$ uptake into OK cells was enhanced only when the cells expressed recombinant CT receptors (Fig. 4), confirming that CRSP-1 enhances the $^{22}Na^{+}$ uptake into the renal epithelial cells through the CT receptor. As for the mechanism of the CRSP-1-induced enhancement of $^{22}Na^{+}$ uptake into LLC-PK$_1$ cells, this effect was abolished by treating with EIPA, an inhibitor of NHE (Fig. 5) [9]. Two isoforms, NHE1 and NHE3, are expressed in LLC-PK$_1$ cells [10,11], and A-kinase is reported to enhance the NHE1-dependent Na^{+} uptake and to suppress the NHE3-dependent Na^{+} uptake [12,13]. Based on these reports, we at first assumed that the effect of CRSP-1 on the Na^{+} uptake shown in Fig. 3 was the summation of the enhancement of the NHE1-dependent Na^{+} uptake and the suppression of the NHE3-dependent Na^{+} uptake. However, Fig. 6 indicates that CRSP-1 selectively activates NHE1 and enhances Na^{+} uptake, which can be explained by the different 50% inhibitory concentrations of EIPA on NHE1 (approximately 1×10^{-8} M) and NHE3 (more than 1×10^{-6} M) [14–17]. At a concentration of 1×10^{-8} M, EIPA can inhibit 30–40% of the $^{22}Na^{+}$ uptake through NHE1 and cannot inhibit it through NHE3, while at a concentration of 1×10^{-6} M EIPA can inhibit more than 95% of the $^{22}Na^{+}$ uptake

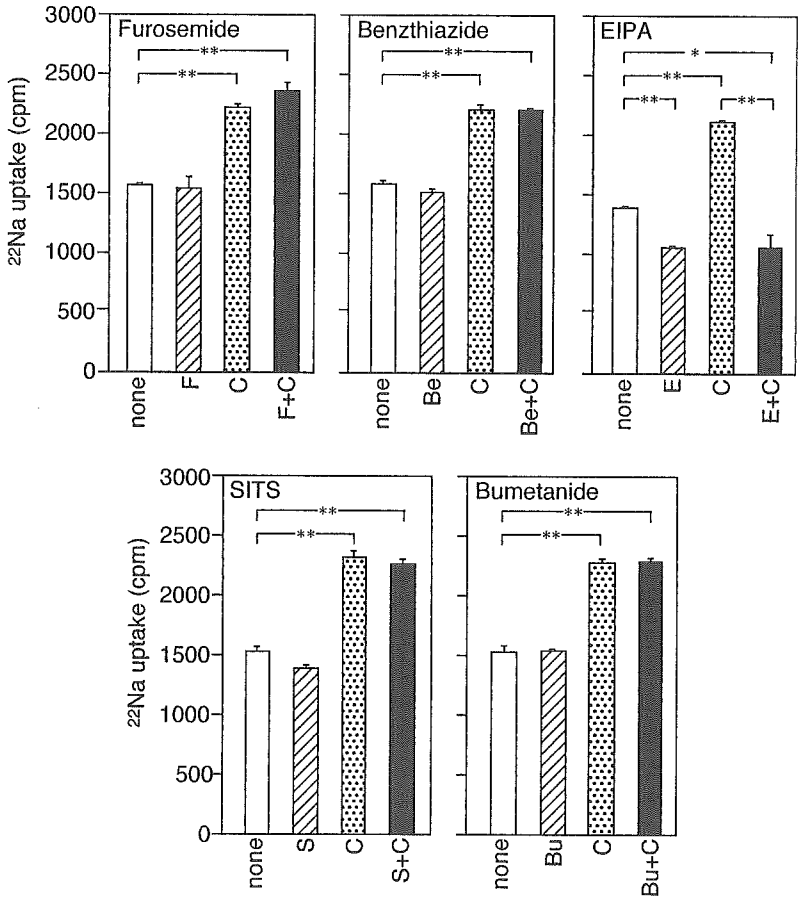

Fig. 5. Effects of ion transporter inhibitors on CRSP-1-induced $^{22}Na^{+}$ uptake into LLC-PK$_1$ cells. LLC-PK$_1$ cells were incubated for 10 min with none (open bar), 1×10^{-6} M of each ion transporter inhibitor (hatched bar), 1×10^{-6} M CRSP-1 (dotted bar), or 1×10^{-6} M CRSP-1 and 1×10^{-6} M of each ion transporter inhibitor (filled bar), in the presence of $^{22}Na^{+}$. C, CRSP-1; F, furosemide; Be, benzthiazide; E, EIPA; S, SITS; and Bu, bumetanide. Each bar represents the mean ± SEM of three separate determinations. $^{**}P < 0.001$.

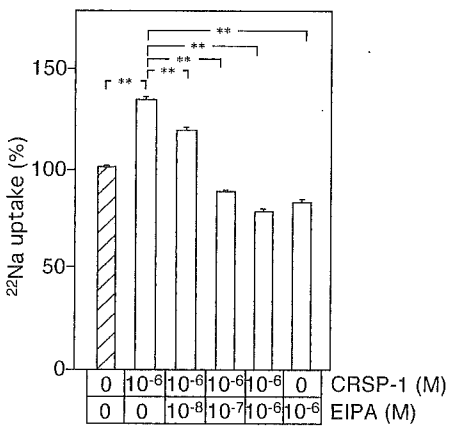

Fig. 6. Dose-dependent inhibitory effect of EIPA on CRSP-1-induced $^{22}Na^{+}$ uptake into LLC-PK$_1$ cells. LLC-PK$_1$ cells were incubated for 10 min with $^{22}Na^{+}$ only (hatched bar), or with $^{22}Na^{+}$ and the indicated concentrations of CRSP-1 and/or EIPA (open bars). Each bar represents the mean ± SEM of three separate determinations. $^{**}P < 0.001$.

through NHE1 and approximately 10% of it through NHE3 [14]. EIPA actually inhibited the CRSP-1-induced enhancement of the $^{22}Na^{+}$ uptake into the LLC-PK$_1$ cells by about 30% at a concentration of 1×10^{-8} M and abolished it at a concentration of 1×10^{-6} M (Fig. 6). This evidence indicates that CRSP-1 enhanced the $^{22}Na^{+}$ uptake into LLC-PK$_1$ cells by activating NHE1 and not by suppressing NHE3 under the present experimental conditions.

NHE1 is localized at the basolateral membrane of the epithelial cells [18,19], and elicits many kinds of cell physiological activities, including the regulation of intracellular pH, cell growth, differentiation, cell migration, and cytoskeletal organization [20]. The data obtained in this study confirmed that CRSP-1 regulates NHE1 activity via the CT receptor-A-kinase pathway in the LLC-PK$_1$ cells, suggesting that this peptide can induce NHE1-mediated cell physiological events in the renal epithelial cells.

On the other hand, the NHE3-dependent Na^{+} uptake into LLC-PK$_1$ (clone 4) cells was reported to be reduced with salmon CT [21], which indicates that CRSP-1 can reduce NHE3 activity by stimulating the CT receptor. In the LLC-PK$_1$ cells used in this study, however, we observed only the stimulatory effect of CRSP-1 on the NHE1 activity instead of observing its inhibitory effect

on the NHE3 activity, probably due to their much lower NHE3 activity than that of NHE1. As NHE3 is localized at the apical membrane of the epithelial cells and is mainly involved in natriuresis, CRSP-1 may be able to regulate the urinary sodium concentration via NHE3 being expressed in the renal epithelial cells.

In conclusion, we investigated the effects of CRSP-1 on the renal epithelial cell line LLC-PK_1, and showed that CRSP-1 enhances the Na^+ uptake mainly through NHE1, reduces the Ca^{2+} uptake, and inhibits the growth of this cell line. Furthermore, these effects of CRSP-1 are stronger than those of porcine CT, which is in agreement with their potencies toward the CT receptor. While the tissue concentration of CRSP-1 in the thyroid gland is estimated to be about 1/10 that of CT [1,22], CRSP-1 is present at a high concentration in the pituitary gland where CT was not detected. These data indicate that the CRSP-1 secreted from these glands can regulate renal epithelial cells in vivo.

Acknowledgments

This work was supported in part by research grants from the Ministry of Education, Culture, Sports, Science and Technology (Special Coordination Funds for the Promotion of Science and Technology), from the Ministry of Health, Labor and Welfare (Cardiovascular Diseases), from the Pharmaceuticals and Medical Devices Agency (Medical Frontier Project) of Japan, and from the Protein Research Foundation (Kaneko-Narita Research Grant). The authors are grateful to Dr. Wakabayashi of this institute for his helpful discussion, and to Ms. A. Okabe, Y. Takada, and S. Fujiwara of this institute for their technical assistance.

References

[1] T. Katafuchi, K. Kikumoto, K. Hamano, K. Kangawa, H. Matsuo, N. Minamino, Calcitonin receptor-stimulating peptide, a new member of the calcitonin gene-related peptide family. Its isolation from porcine brain, structure, tissue distribution, and biological activity, J. Biol. Chem. 278 (2003) 12046–12054.

[2] R.N. Hull, W.R. Cherry, G.W. Weaver, The origin and characteristics of a pig kidney cell strain, LLC-PK, In Vitro 12 (1976) 670–677.

[3] A. Perantoni, J.J. Berman, Properties of Wilms' tumor line (TuWi) and pig kidney line (LLC-PK_1) typical of normal kidney tubular epithelium, In Vitro 15 (1979) 446–454.

[4] J.S. Handler, F.M. Perkins, J.P. Johnson, Studies of renal cell function using cell culture techniques, Am. J. Physiol. 238 (1980) F1–F9.

[5] H.Y. Lin, T.L. Harris, M.S. Flannery, A. Aruffo, E.H. Kaji, A. Gorn, L.F. Kolakowski Jr., H.F. Lodish, S.R. Goldring, Expression cloning of an adenylate cyclase-coupled calcitonin receptor, Science 254 (1991) 1022–1024.

[6] D.A. Jans, E.L. Gajdas, C. Dierks-Ventling, B.A. Hemmings, F. Fahrenholz, Long-term stimulation of cAMP production in LLC-PK_1 pig kidney epithelial cells by salmon calcitonin or a photoactivatable analogue of vasopressin, Biochim. Biophys. Acta 930 (1987) 392–400.

[7] A. Inoue, Y. Komatsu, J. Ochiai, S. Itagaki, H. Nishide, M. Shikano, H. Hemmi, N. Numao, Growth inhibition and morphological changes of LLC-PK_1 induced by ultimobranchial calcitonins, Cell Biol. Int. Rep. 14 (1990) 887–896.

[8] R.J. Bindels, Calcium handling by the mammalian kidney, J. Exp. Biol. 184 (1993) 89–104.

[9] S. Wakabayashi, M. Shigekawa, J. Pouyssegur, Molecular physiology of vertebrate Na^+/H^+ exchangers, Physiol. Rev. 77 (1997) 51–74.

[10] R.F. Reilly, F. Hildebrandt, D. Biemesderfer, C. Sardet, J. Pouyssegur, P.S. Aronson, C.W. Slayman, P. Igarashi, cDNA cloning and immunolocalization of a $Na^{(+)}$–H^+ exchanger in LLC-PK_1 renal epithelial cells, Am. J. Physiol. 261 (1991) F1088–F1094.

[11] C.A. Shugrue, N. Obermuller, S. Bachmann, C.W. Slayman, R.F. Reilly, Molecular cloning of NHE3 from LLC-PK_1 cells and localization in pig kidney, J. Am. Soc. Nephrol. 10 (1999) 1649–1657.

[12] R.A. Kandasamy, F.H. Yu, R. Harris, A. Boucher, J.W. Hanrahan, J. Orlowski, Plasma membrane Na^+/H^+ exchanger isoforms (NHE-1, -2, and -3) are differentially responsive to second messenger agonists of the protein kinase A and C pathways, J. Biol. Chem. 270 (1995) 29209–29216.

[13] A. Azarani, J. Orlowski, D. Goltzman, Parathyroid hormone and parathyroid hormone-related peptide activate the Na^+/H^+ exchanger NHE-1 isoform in osteoblastic cells (UMR-106) via a cAMP-dependent pathway, J. Biol. Chem. 270 (1995) 23166–23172.

[14] J. Orlowski, Heterologous expression and functional properties of amiloride high affinity (NHE-1) and low affinity (NHE-3) isoforms of the rat Na/H exchanger, J. Biol. Chem. 268 (1993) 16369–16377.

[15] F.H. Yu, G.E. Shull, J. Orlowski, Functional properties of the rat Na/H exchanger NHE-2 isoform expressed in Na/H exchanger-deficient Chinese hamster ovary cells, J. Biol. Chem. 268 (1993) 25536–25541.

[16] M. Kuwahara, S. Sasaki, S. Uchida, E.J.J. Cragoel, F. Marumo, Different development of apical and basolateral Na–H exchangers in LLC-PK_1 renal epithelial cells: characterization by inhibitors and antisense oligonucleotide, Biochim. Biophys. Acta 1220 (1994) 132–138.

[17] J. Orlowski, R.A. Kandasamy, Delineation of transmembrane domains of the Na^+/H^+ exchanger that confer sensitivity to pharmacological antagonists, J. Biol. Chem. 271 (1996) 19922–19927.

[18] B. Coupaye-Gerard, C. Bookstein, P. Duncan, X.Y. Chen, P.R. Smith, M. Musch, S.A. Ernst, E.B. Chang, T.R. Kleyman, Biosynthesis and cell surface delivery of the NHE1 isoform of Na^+/H^+ exchanger in A6 cells, Am. J. Physiol. 271 (1996) C1639–C1645.

[19] J. Noel, D. Roux, J. Pouyssegur, Differential localization of Na^+/H^+ exchanger isoforms (NHE1 and NHE3) in polarized epithelial cell lines, J. Cell Sci. 109 (1996) 929–939.

[20] E. Slepkov, L. Fliegel, Structure and function of the NHE1 isoform of the Na^+/H^+ exchanger, Biochem. Cell Biol. 80 (2002) 499–508.

[21] M. Chakraborty, D. Chatterjee, F.S. Gorelick, R. Baron, Cell cycle-dependent and kinase-specific regulation of the apical Na/H exchanger and the Na,K-ATPase in the kidney cell line LLC-PK_1 by calcitonin, Proc. Natl. Acad. Sci. USA 91 (1994) 2115–2119.

[22] L.J. Deftos, M.R. Lee, J.T.J. Potts, A radioimmunoassay for thyrocalcitonin, Proc. Natl. Acad. Sci. USA 60 (1968) 293–299.

Available online at www.sciencedirect.com
SCIENCE DIRECT®
ELSEVIER
Peptides 26 (2005) 2616–2623
PEPTIDES
www.elsevier.com/locate/peptides

Isolation and characterization of a glycine-extended form of calcitonin receptor-stimulating peptide-1: Another biologically active form of calcitonin receptor-stimulating peptide-1

Takeshi Katafuchi, Kazumasa Hamano, Katsuro Kikumoto, Naoto Minamino *

Department of Pharmacology, National Cardiovascular Center Research Institute, 5-7-1 Fujishirodai, Suita, Osaka 565-8565, Japan

Received 25 March 2005; received in revised form 4 June 2005; accepted 6 June 2005
Available online 14 July 2005

Abstract

In this study, we isolated a peptide eliciting a potent stimulatory effect on cAMP production in LLC-PK_1 cells from acid extracts of porcine brain. By structural analysis, this peptide was determined to be a C-terminal glycine-extended form of calcitonin receptor-stimulating peptide-1 (CRSP-1-Gly). Synthetic CRSP-1-Gly enhanced the cAMP production in COS-7 cells expressing calcitonin (CT) receptor as strongly as CRSP-1. Measurement of immunoreactive (IR) CRSP-1-Gly by radioimmunoassay using the specific antisera against CRSP-1-Gly showed that a relatively high level (>1 pmol/g wet weight) of IR-CRSP-1-Gly was detected in the midbrain, hypothalamus, anterior and posterior lobes of pituitary, and thyroid gland, and the ratio of IR-CRSP-1-Gly to total IR-CRSP-1 varies from 0.02 to 0.35 in each tissue. These results suggest that CRSP-1-Gly is actually present in the tissues as one of major endogenous molecular forms of CRSP-1, and can regulate the cells expressing the CT receptor both in the central nervous system and peripheral tissues in a manner similar to that of CRSP-1. IR-CRSP-2 and IR-CRSP-3 are also present in the brain and other tissues, but their tissue concentrations are 33% on average and less than 3% that of total IR-CRSP-1, respectively.

Keywords: Calcitonin receptor-stimulating peptide; Glycine-extended form of calcitonin receptor-stimulating peptide; Isolation; Calcitonin receptor; cAMP; Radioimmunoassay

1. Introduction

We have reported the structure, tissue expression and biological activity of three calcitonin receptor-stimulating peptides (CRSPs) in the pig [10,12]. Among them, the biological features of CRSP-1 have been characterized in greater detail. CRSP-1 exists in the central nervous system (CNS), pituitary and thyroid gland, and stimulates the calcitonin (CT) receptor about 100-fold more potently than CT. These facts indicate that CRSP-1 is a strong and specific ligand for the CT receptor expressing both in the CNS and peripheral tissues.

CRSP-1 was isolated from acid extracts of porcine brain by monitoring cAMP production through the endogenously expressing CT receptor expressed in LLC-PK_1 cells [9,12,15]. In the preceding study of CRSP-1 purification, six major peaks of the cAMP producing activity were observed in CM-52 ion exchange chromatography of the strongly basic peptides prepared from the porcine brain extracts [12]. Among them, CRSP-1 was isolated from the sixth peak of the cAMP producing activity, while we have identified the first three peaks as calcitonin gene-related peptide (CGRP) and its related peptides by further purification and structural analysis. In the present study, we successfully purified a new biologically active peptide from the fractions corresponding to the fifth peak of the cAMP producing activity in the CM-52 ion exchange chromatography, and determined it to be a glycine-extended and non-amidated form of CRSP-1 (CRSP-1-Gly) by structural analysis. Here we report the

* Corresponding author. Tel.: +81 6 6833 5012x2507; fax: +81 6 6835 5349.
E-mail address: minamino@ri.ncvc.go.jp (N. Minamino).

0196-9781/$ – see front matter © 2005 Elsevier Inc. All rights reserved.
doi:10.1016/j.peptides.2005.06.004

purification and biological activity of CRSP-1-Gly. Tissue concentrations of immunoreactive (IR) CRSP-1-Gly in the porcine tissues were also measured using a specific antiserum and compared with those of IR-CRSP-1, IR-CRSP-2 and IR-CRSP-3.

2. Materials and methods

2.1. Peptides

CRSP-1 was synthesized as described previously [12]. CRSP-1-Gly, N-Tyr-CRSP-1[30–38]-Gly and N-Cys-CRSP-1[30–38]-Gly were custom synthesized by American Peptide Company (Sunnyvale, CA). N-Tyr-CRSP-2[29–37]-NH_2, N-Cys-CRSP-2[29–37]-NH_2, N-Tyr-CRSP-3[29–37]-NH_2 and N-Cys-CRSP-3[29–37]-NH_2 were custom synthesized by Peptide Institute (Osaka, Japan). The purity and amino acid sequence were evaluated and confirmed using C_{18} reverse phase HPLC, amino acid analyzer and protein sequencer.

2.2. Measurement of cAMP production

COS-7 cells and LLC-PK_1 cells were maintained as reported previously [12], plated at 100,000 cells/well on 48-well plates and cultured for 24 h. The porcine CT receptor cDNA ligated into pcDNA 3.1 expression vector (Promega, Madison, WI) was transfected into the COS-7 cells with Lipofectamine Plus (Invitrogen Life Technologies, Carlsbad, CA) according to the manufacturer's protocol [13]. Both LLC-PK_1 and COS-7 cells that were recombinantly expressing the CT receptor were washed twice with Dulbecco's modified Eagle's medium (DMEM)/Hepes (20 mM, pH 7.4) containing 0.5 mM 3-isobutyl-1-methyl xanthine (Sigma, St Louis, MO) and 0.05% bovine serum albumin (BSA), and incubated in the same medium for 30 min at 37 °C. The incubation medium was then replaced with 150 μl of medium, in which the sample of interest was dissolved, and further incubated at 37 °C for another 30 min. Aliquots (100 μl) of the incubation media were succinylated, evaporated, and then submitted to radioimmunoassay (RIA) for cAMP, as reported previously [12].

2.3. Isolation of CRSP-1-Gly

The basic peptide fraction (SP-III) with molecular mass of about 3 kDa was prepared from porcine brain extracts as described previously [12]. This strongly basic peptide fraction was subjected to carboxymethyl (CM) ion exchange chromatography (CM-52, 2.4 cm × 45 cm; Whatman, Clifton, NJ) eluting with a linear gradient elution of $HCOONH_4$ (pH 6.5) from 9 mM to 0.45 M containing 10% CH_3CN. In the course of the present purification, aliquots (1/2000) of all fractions were lyophilized, dissolved in 200 μl of incubation medium, and submitted to the measurement of the cAMP producing activity using LLC-PK_1 cells. The fractions eliciting cAMP-producing activity were pooled and re-purified by cation exchange high performance liquid chromatography (HPLC) (TSK-gel CM-2SW, 7.8 mm × 300 mm; Tosoh, Tokyo, Japan) eluting with a linear gradient elution of $HCOONH_4$ (pH 3.8) from 9 mM to 0.9 M containing 10% CH_3CN at a flow rate of 2 ml/min. The biologically active fractions were successively separated by reverse phase HPLC on a C_{18} column (218TP54, 4.6 mm × 250 mm; Vydac, Hesperia, CA), and on a diphenyl column (219TP5215, 2.1 mm × 150 mm; Vydac) using a linear gradient elution of CH_3CN from 10 to 60% in 0.1% trifluoroacetic acid (TFA) at flow rates of 1 and 0.2 ml/min, respectively. The amino acid sequence was analyzed with a Procise cLC protein sequencer (492, Applied Biosystems, Foster City, CA), and mass spectra were measured using a single quadrupole mass spectrometer with electrospray ionization source (SSQ 7000, Finnigan, San Jose, CA) as described previously [12].

2.4. Preparation of antisera against CRSP-1-Gly, CRSP-2 and CRSP-3

All experimental procedures were approved by the local animal experiments and care committee. Rabbit antisera were raised against CRSP-1[30–38]-Gly, CRSP-2[29–37]-NH_2 and CRSP-3[29–37]-NH_2, to each of which an N-terminal cysteine was added to facilitate specific conjugation to maleimide-activated keyhole limpet hemocyanin through the sulfhydryl group of cysteine (Pierce, Rockford, IL). New Zealand White rabbits (Japan SLC, Hamamatsu, Japan) were immunized by injecting 1 mg of each peptide-keyhole limpet hemocyanin conjugate emulsified in complete Freund's adjuvant, and antibody production was boosted by five additional injections of the antigen conjugate emulsion at 3-week intervals.

2.5. Measurement of IR-CRSP-1-Gly, IR-CRSP-1, IR-CRSP-2 and IR-CRSP-3 concentrations in the porcine brain, pituitary and thyroid gland by RIA

N-Tyr-CRSP-1[30–38]-Gly, N-Tyr-CRSP-1[24–38]-NH_2, N-Tyr-CRSP-2[29–37]-NH_2 and N-Tyr-CRSP-3[29–37]-NH_2 were each radioiodinated by the lactoperoxidase method, and each monoiodinated peptide was isolated by reverse phase HPLC. Approximately 1 g of porcine tissue was minced and boiled for 10 min in 5 ml of water. After cooling, water and acetic acid were added to a final volume and concentration of 10 ml and 1 M, respectively, and the boiled tissues were homogenized with a Polytron homogenizer. The homogenates were then centrifuged, and 1 ml of the resulting supernatant was lyophilized, dissolved in the 1 ml of RIA buffer (50 mM sodium phosphate (pH 7.4), containing 80 mM NaCl, 25 mM EDTA, 0.05% NaN_3, 0.5% BSA treated with N-ethylmaleimide, and 0.5% Triton X-100). An aliquot (100 μl) of the solution was submitted to each RIA, which was performed by the procedures described previously [12].

2.6. Characterization of IR-CRSP-1 and IR-CRSP-1-Gly in the porcine brain

The SP-III fraction of porcine brain extracts was lyophilized, dissolved in 60% CH_3CN containing 0.1% TFA and was equally divided into four portions. Each portion was separated by gel filtration HPLC (TSK-G2000 SW_{XL}, 7.8 mm × 300 mm; Tosoh) eluting with 60% CH_3CN containing 0.1% TFA at a flow rate of 0.2 ml/min, and the effluent was collected into the same tube set. One-fifth of each fraction was lyophilized, dissolved in the RIA buffer, and aliquots (100 μl) were submitted for RIAs for CRSP-1 and CRSP-1-Gly. The fractions containing IR-CRSP-1 or IR-CRSP-1-Gly were pooled, divided into two equal portions, and lyophilized. For the reverse phase HPLC, the half portion was dissolved in 10% CH_3CN containing 0.1% TFA and separated by a C_{18} column (Symmetry 300™ C_{18} 5 μm, 4.6 mm × 250 mm; Waters) using a linear gradient elution of CH_3CN from 10 to 60% containing 0.1% TFA at a flow rate of 1 ml/min. For the ion exchange HPLC, another half portion of the sample was dissolved with 9 mM $HCOONH_4$ (pH 6.5) containing 10% CH_3CN, and separated by CM ion exchange HPLC (TSK-gel CM-2SW, 7.8 mm × 300 mm; Tosoh) eluting with a linear gradient elution of $HCOONH_4$ (pH 6.5) from 9 mM to 0.9 M containing 10% CH_3CN at 2 ml/min. The whole fractions were lyophilized, eliminated $HCOONH_4$ by sublimation, dissolved in the RIA buffer (1 ml), and aliquots (100 μl) were submitted to RIAs for CRSP-1 and CRSP-1-Gly.

3. Results

3.1. Isolation and sequence determination of CRSP-1-Gly

Fig. 1A shows the absorbance and cAMP-producing activity of each fraction in the CM-52 cation exchange chromatography of the basic peptide fraction of about 3 kDa prepared from porcine brain extracts. At least six major peaks of stimulatory activity in the cAMP production assay were observed, and we previously purified peptides from peaks 1–3 and 6. Amino acid sequences of the peptides isolated from peaks 1–3 were determined from the N-termini to more than the 15th residues, which were identical with that of CGRP. Based on the sequencing data along with the elution positions of synthetic CGRP and its methionine sufoxide form in reverse phase HPLC, we deduced that three peaks eliciting the cAMP-producing activity were a methionine sufoxide form of CGRP, CGRP and an unidentified CGRP-derived peptide, respectively. On the other hand, CRSP-1 was isolated from peak 6 as shown in our preceding study [12]. The biologically active fractions corresponding to peak 5 were pooled, and first separated by CM ion exchange HPLC on a TSK-gel CM-2SW column using a buffer of different pH, and then purified by reverse phase HPLC on a C_{18} column. Final purification was performed by another reverse phase

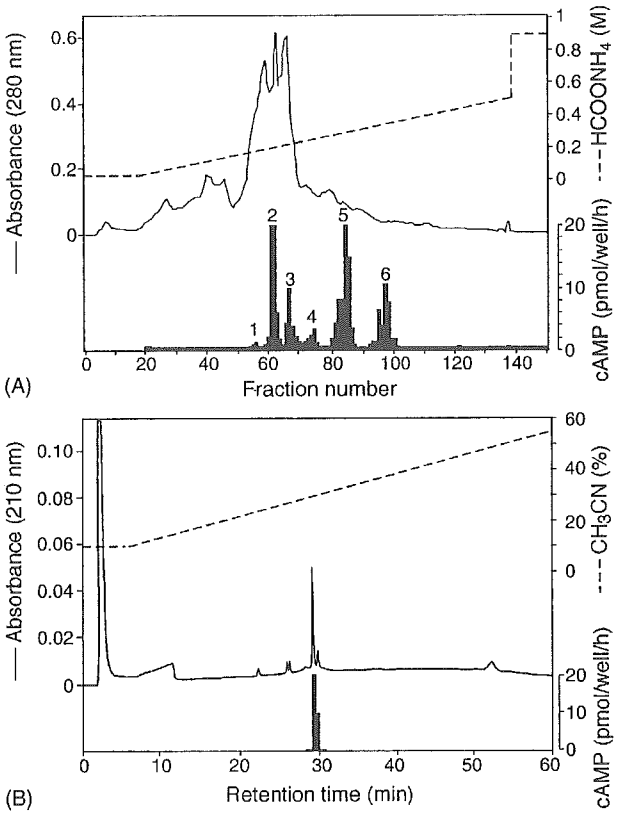

Fig. 1. Purification of CRSP-1-Gly from porcine brain extracts. (A) CM ion exchange chromatography of the basic peptide fraction prepared from porcine brain extracts. Sample: Basic peptides of molecular masses of 3 kDa obtained by successive Sephadex G-50 and G-25 gel filtrations from SP-III fraction of porcine brain extracts. Column, CM-52 (24 mm × 450 mm, Whatman); fraction size, 20 ml/tube; flow rate, 35 ml/h. Solvent system: linear gradient elution of $HCOONH_4$ (pH 6.5) from 9 mM to 0.45 M in 10% CH_3CN (v/v). (B) Final purification of CRSP-1-Gly by reverse phase HPLC. Sample: Biologically active fraction obtained by C_{18} reverse phase HPLC. Column, diphenyl (2.1 mm × 150 mm, Vydac 219TP5215); flow rate, 0.2 ml/min. Solvent system: Linear gradient elution of CH_3CN from 10 to 60% in 0.1% TFA (v/v) for 60 min. An aliquot of each fraction of (A) and (B) was submitted to the bioassay of cAMP producing activity in LLC-PK_1 cells.

HPLC on a diphenyl column, and the peptide was purified to a homogenous state (Fig. 1B).

To determine the amino acid sequence, intact and tryptic fragments of the purified peptide were subjected to the N-terminal sequence analysis using a protein sequencer. Contrary to our expectation, the amino acid sequences of the intact peptide and tryptic fragments were completely identical to those of CRSP-1, and the amino acid sequence of the purified peptide was confirmed up to the 37th residue. To determine the precise molecular mass, the purified peptide was analyzed using an ESI mass spectrometer, and its molecular mass was determined to be 4189.5 ± 0.3 Da. On the other hand, the molecular mass of CRSP-1 purified from peak 6 was determined to be 4130.6 ± 0.7 Da in the preceding study as two methionines of CRSP-1 (intact molecular mass 4098.9 Da) were oxidized to methionine sulfoxides (plus 16.0 Da × 2). As the difference of molecular

masses between the purified peptide and the methionine sulfoxide form of CRSP-1 was 58.9 Da, we hypothesized that the C-terminal glycine is retained intact without being converted into the amide in the peptide purified in this study. To verify whether the peptide purified from peak 5 is the glycine-extended form of CRSP-1 (CRSP-1-Gly), we synthesized CRSP-1-Gly and compared the retention times of CRSP-1-Gly possessing two methionine sulfoxides with those of the purified peptide in the ion exchange and the reverse phase HPLCs. We concluded that the purified peptide was the glycine-extended form of CRSP-1, based on its retention times in the two HPLCs (data not shown).

3.2. Effects of CRSP-1-Gly on the porcine CT receptor

To compare the biological potency of synthetic CRSP-1-Gly with that of CRSP-1 on the CT receptor, we stimulated LLC-PK_1 cells as well as COS-7 cells expressing porcine CT receptor with CRSP-1-Gly or CRSP-1, and measured their cAMP production levels. As shown in Fig. 2, the dose-response curve of CRSP-1-Gly overlapped with that of CRSP-1 both in LLC-PK_1 cells and in the COS-7 cells expressing the CT receptor, indicating that CRSP-1-Gly is equipotent as CRSP-1. Although there is a possibility that CRSP-1-Gly acts on the CT receptor after conversion into CRSP-1 by alpha-amidating monooxygenase (PAM), COS-7 cells are reported to have an undetectable level of the PAM activity [24]. These data indicate that CRSP-1-Gly can directly stimulate the CT receptor even though it does not have the amide structure.

3.3. Characterization of IR-CRSP-1-Gly and IR-CRSP-1 in the porcine brain

IR-CRSP-1-Gly and IR-CRSP-1 levels in the porcine brain extracts were measured using the antiserum against CRSP-1[24–38]-NH_2 prepared in our previous study [12] and a newly prepared antiserum against CRSP-1[30–38]-Gly. Half-maximal inhibition of radioiodinated ligand binding to the antiserum against CRSP-1[30–38]-Gly was observed at 20 fmol/tube. The antisera against CRSP-1[24–38]-NH_2 and CRSP-1[30–38]-Gly have very low cross-reactivity with CRSP-1-Gly and CRSP-1, respectively (<0.1%). The acid extracts of porcine whole brain without cerebellum were separated by gel filtration HPLC, reverse phase HPLC and ion exchange HPLC, and IR-CRSP-1-Gly and IR-CRSP-1 levels in each fraction were measured using RIAs specific for CRSP-1 and CRSP-1-Gly. The retention time of IR-CRSP-1-Gly was almost identical to that of IR-CRSP-1 in the gel filtration HPLC, as molecular masses of CRSP-1-Gly (4156.9 Da) and CRSP-1 (4098.9 Da) are almost identical with each other (Fig. 3). Similarly, the retention time of IR-CRSP-1-Gly was almost identical to that of IR-CRSP-1 in the reverse phase HPLC (Fig. 4), as the conversion of the C-terminal glycine of CRSP-1-Gly into the amide did not affect their hydrophobicity in the reverse phase HPLC under the acidic conditions. On the other hand, this C-terminal conversion increased the retention time in the CM-2SW ion exchange HPLC (Fig. 5), as the C-terminal glycine of CRSP-1-Gly carries a negative charge in the neutral pH range. The peak height of IR-CRSP-1-Gly in each HPLC was approximately 30% of that of IR-CRSP-1. This fact suggests that about one-fourth of total IR-CRSP-1 (IR-CRSP-1 plus IR-CRSP-1-Gly) is IR-CRSP-1-Gly in the porcine brain. Compared to other neuropeptides, IR-CRSP-1 and IR-CRSP-1-Gly were eluted relatively in wide ranges in each HPLC, particularly in the gel filtration HPLC and ion exchange HPLC. The wide spread elution of these immunoreactivity in the gel filtration HPLC may be due to the overload of the sample. On the other hand, the wide spread elution of the immunoreactivity in the ion exchange HPLC is probably due to the oxidation of three methionines in the sequences of CRSP-1 and CRSP-1-Gly.

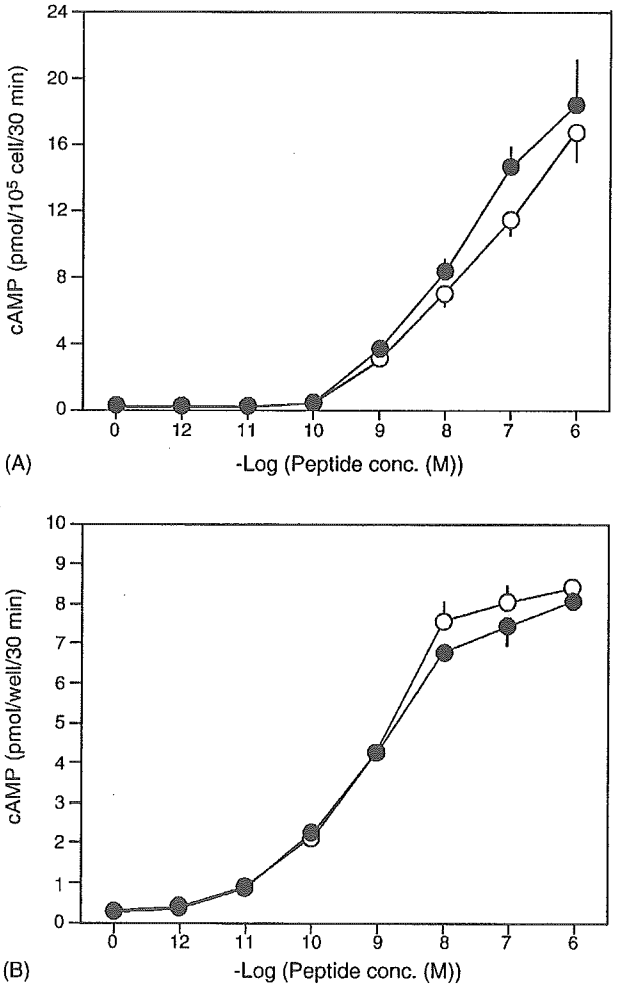

Fig. 2. Effects of CRSP-1 and CRSP-1-Gly on cAMP production in LLC-PK_1 cells (A), and COS-7 cells expressing porcine CT receptor (B). LLC-PK_1 cells as well as COS-7 cells expressing the porcine CT receptor were stimulated with the indicated concentrations of CRSP-1 (open circle) and CRSP-1-Gly (closed circle). The assay media were then succinylated, evaporated, and submitted to RIA for cAMP. Each point represents the mean ± S.E.M. of three separate determinations.

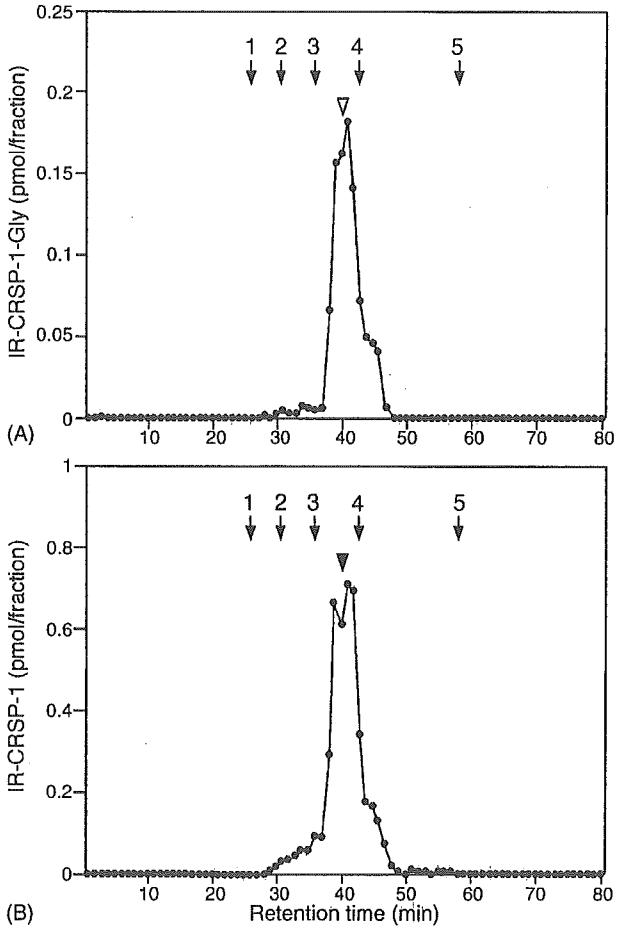

Fig. 3. Gel filtration HPLC of porcine brain extracts. The SP-III fraction of porcine brain extracts was separated by gel filtration HPLC on a TSK-gel G2000SW$_{XL}$ column (7.8 mm × 300 mm, Tosoh), eluting with 60% CH_3CN containing 0.1% TFA at a flow rate of 0.2 ml/min. Aliquots of each fraction were submitted to RIAs for CRSP-1 (A) and CRSP-1-Gly (B). Arrowheads indicate the retention times of synthetic CRSP-1-Gly (open arrowhead) and CRSP-1 (closed arrowhead). Arrows indicate the retention times of (1) BSA, (2) horse myoglobin, (3) human adrenomedullin, (4) neurotensin, and (5) acetic acid.

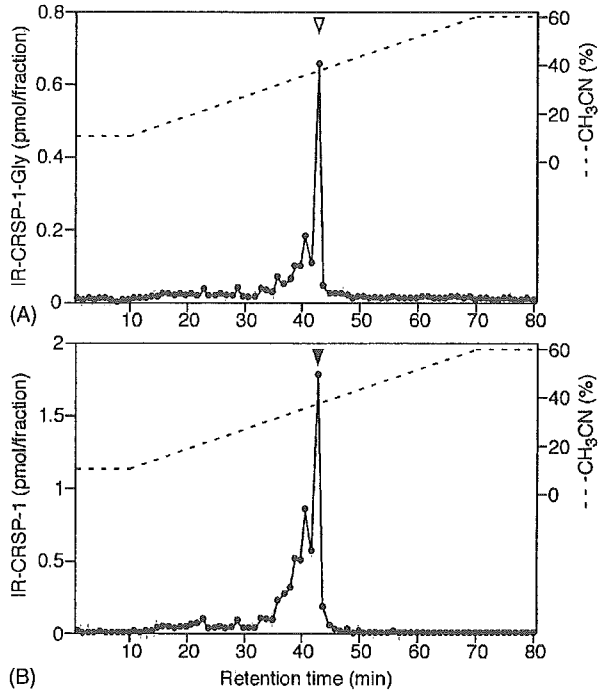

Fig. 4. Reverse phase HPLC of porcine brain extracts. Peak fractions of IR-CRSP-1 and IR-CRSP-1-Gly eluted from the gel filtration HPLC (Fig. 3) were pooled, lyophilized, and separated by reverse phase HPLC on a C_{18} column (Symmetry 300^{TM} C_{18} 5 μm, 4.6 mm × 250 mm; Waters) using a linear gradient elution of CH_3CN from 10 to 60% in 0.1% TFA at a flow rate of 1 ml/min. Aliquots of each fraction were submitted to RIAs for CRSP-1 (A) and CRSP-1-Gly (B). Arrowheads indicate the retention times of synthetic CRSP-1-Gly (open arrowhead) and CRSP-1 (closed arrowhead).

In fact, two methionines of CRSP-1 and CRSP-1-Gly were oxidized when we isolated them, indicating that at least two of three methionines are easily oxidized during the extraction and purification. We deduce that CRSP-1 and CRSP-1-Gly are not oxidized in the brain tissue, but that they are oxidized in the steps of extraction and separation.

3.4. Measurement of concentrations of IR-CRSP-1-Gly, IR-CRSP-1, IR-CRSP-2 and IR-CRSP-3 in porcine tissues

We next evaluated the tissue levels of IR-CRSP-1-Gly and IR-CRSP-1, using the antisera specific for each peptide. In addition, we prepared antisera against CRSP-2[29–37]-NH_2 and CRSP-3[29–37]-NH_2 to measure the tissue concentrations of CRSP-2 and CRSP-3. Half-maximal inhibition of radioiodinated ligand binding to antisera against CRSP-2[29–37]-NH_2 or CRSP-3[29–37]-NH_2 was observed at 20 fmol/tube or 50 fmol/tube, respectively, and their N-terminal extensions, i.e. CRSP-2 and CRSP-3, did not alter sensitivity of each RIA. The antisera against CRSP-1[24–38]-NH_2, CRSP-1[30–38]-Gly, CRSP-2[29–37]-NH_2 and CRSP-3[29–37]-NH_2 have very low cross-reactivity with all these antigens (<0.1%) except for each antigen used for the immunization. Using these antisera, we measured the tissue concentrations of IR-CRSP-1-Gly, IR-CRSP-1, IR-CRSP-2 and IR-CRSP-3, and calculated the ratio in the tissue concentration of IR-CRSP-1-Gly to total IR-CRSP-1 (Table 1). More than 0.2 pmol/g wet tissue of IR-CRSP-1-Gly was detected in all tissues except for the cerebellum. More than 1 pmol/g wet tissue of IR-CRSP-1-Gly was detected in the midbrain, hypothalamus, anterior and posterior lobes of pituitary and thyroid gland, where a relatively high concentration of CRSP-1 was observed (>6 pmol/g wet tissue). The highest concentration of IR-CRSP-1-Gly was detected in the posterior lobe of pituitary (5.39 ± 0.57 pmol/g wet tissue). The ratio of IR-CRSP-1-Gly to the total IR-CRSP-1 varies from 0.02 to 0.35, and the highest ratio (0.35) was observed in the hippocampus and olfactory bulb.

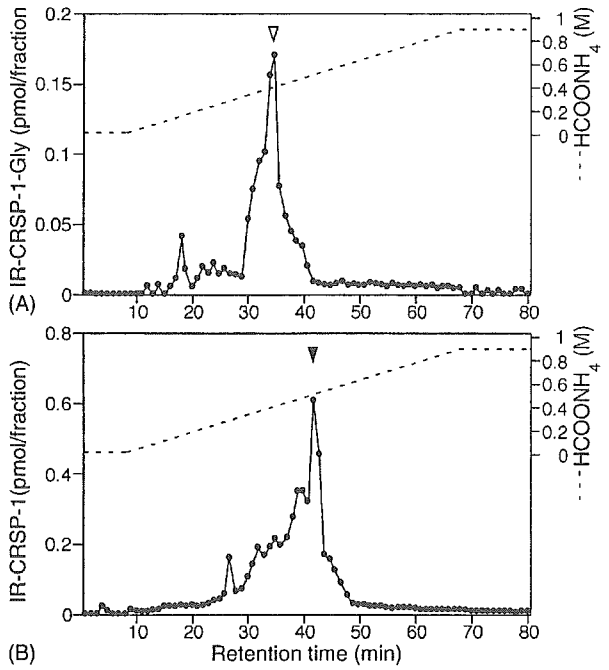

Fig. 5. Cation exchange HPLC of porcine brain extracts. Peak fractions of CRSP-1 and CRSP-1-Gly eluted from the gel filtration HPLC (Fig. 3) were pooled, lyophilized, and separated by CM ion exchange HPLC (TSK-gel CM-2SW, 7.8 mm × 300 mm; Tosoh) eluting with a linear gradient elution of $HCOONH_4$ (pH 6.5) from 9 mM to 0.9 M containing 10% CH_3CN at a flow rate of 2 ml/min. Aliquots of each fraction were lyophilized and submitted to RIAs for CRSP-1 (A) and CRSP-1-Gly (B). Arrowheads indicate the retention times of synthetic CRSP-1-Gly (open arrowhead) and CRSP-1 (closed arrowhead).

On the other hand, more than 1 pmol/g wet tissue of IR-CRSP-2 was observed in the midbrain, hypothalamus, anterior and posterior lobes of pituitary and thyroid gland, and the tissue concentrations of IR-CRSP-2 were comparable to those of IR-CRSP-1-Gly. However, significant levels of IR-CRSP-3 were observed only in the anterior and posterior lobes of pituitary and hypothalamus, and those in the other brain regions were less than the limit of quantitative measurement.

4. Discussion

Many biologically active peptides possess the C-terminal amide structure, and in most of the amidated peptides, such as oxytocin [7], gastrin [17], thyrotropin releasing hormone [19] and CT [22], the C-terminal amide structure is shown to be essential for eliciting their full biological activity. These facts imply that the strong interaction exists between the C-terminal amide structure of these peptides and the ligand binding site of their receptors. As shown in Fig. 2, however, we demonstrated that the glycine-extended form of CRSP-1 is as potent as CRSP-1 on both the endogenously expressed and recombinantly expressed CT receptors. This result indicates that no interaction exists between the C-terminal end of CRSP-1 and the ligand binding site of the CT receptor. We have already shown that the precursors of bovine and canine CRSP-1s do not have a donor glycine for the amidation, but synthetic bovine and canine CRSP-1s lacking the C-terminal amide can stimulate the CT receptor at a potency comparable to that of amidated porcine CRSP-1 [11]. In the limited cases of the amidated peptides, such as vasointestinal polypeptide [6,8], PHI [5] and secretin [18] of the same peptide family, the C-terminal amide structure is not essential for eliciting their activity. CRSP-1 is considered to belong to this exceptional case, and is the first exception in the CGRP family, as the C-terminal amidation is essential for eliciting its activity in the other members of the CGRP family [4,14,22,23].

Relatively high concentrations of IR-CRSP-1-Gly were detected in the tissues and brain regions, such as the midbrain, hypothalamus, anterior and posterior lobes of pituitary and thyroid gland (>1 pmol/g wet tissue), where high concentrations of IR-CRSP-1 (>6 pmol/g wet tissue) were also observed (Table 1). Based on these results, the relative ratio in the tissue concentration of IR-CRSP-1-Gly to total IR-CRSP-1 was calculated to be 0.02–0.35 in each region and tissue. The ratio of IR-CRSP-1-Gly to total IR-CRSP-1 was the lowest in the posterior lobe of pituitary and thyroid gland, which contained the highest levels of IR-CRSP-1 (>60 pmol/g wet weight). In contrast, all brain regions and the anterior lobe of pituitary contain IR-CRSP-1-Gly at higher

Table 1
Concentrations (pmol/g wet weight) of IR-CRSP-1-Gly, IR-CRSP-1, IR-CRSP-2 and IR-CRSP-3 in porcine tissues, and ratio of IR-CRSP-1-Gly to total IR-CRSP-1

Tissue	CRSP-1-Gly	CRSP-1	CRSP-2	CRSP-3	CRSP-1-Gly/total CRSP-1
Cerebral cortex	<0.2	0.33 ± 0.01	0.27 ± 0.04	<0.2	ND
Cerebellum	0.21 ± 0.05	<0.2	0.46 ± 0.23	<0.2	ND
Midbrain	1.40 ± 0.04	7.53 ± 0.72	1.02 ± 0.20	<0.2	0.16
Hippocampus	0.51 ± 0.04	0.97 ± 0.04	0.38 ± 0.11	<0.2	0.35
Caudate nucleus	0.49 ± 0.04	1.31 ± 1.67	0.69 ± 0.19	<0.2	0.27
Thalamus	0.70 ± 0.4	3.67 ± 0.11	0.71 ± 0.20	<0.2	0.16
Hypothalamus	1.44 ± 0.07	6.57 ± 1.21	1.25 ± 0.23	0.20 ± 0.04	0.18
Pons/medulla oblongata	0.53 ± 0.01	1.86 ± 0.20	0.42 ± 0.10	<0.2	0.22
Olfactory bulb	0.24 ± 0.04	0.45 ± 0.06	0.45 ± 0.14	<0.2	0.35
Pituitary, anterior	2.50 ± 0.11	11.56 ± 1.44	1.29 ± 0.34	0.67 ± 0.08	0.18
Pituitary, posterior	5.39 ± 0.57	109.88 ± 25.99	4.56 ± 0.45	2.85 ± 0.52	0.05
Thyroid gland	1.33 ± 0.37	66.78 ± 26.19	1.46 ± 0.75	<0.2	0.02

Each value represents mean ± S.E.M. ($n = 3$). ND, not determined.

ratios of 0.16–0.35. Consistent with these ratios, the peak height of IR-CRSP-1-Gly observed in each HPLC of the characterization (Figs. 3–5) was approximately 30% that of IR-CRSP-1, indicating that CRSP-1-Gly is present as one of the major endogenous forms and can act on the cells expressing CT receptor. In the hypothalamus, pituitary and thyroid gland, PAM is known to be abundantly expressed [1,2,16,20,21]. On the other hand, the conversion rate of Tyr-Gly-Gly into Tyr-Gly-amide by PAM was reported to be much lower than that of Tyr-X-Gly into Tyr-X-amide (X = aromatic or aliphatic residue) [3]. To elucidate the differences in the ratio of CRSP-1 to CRSP-1-Gly in each tissue and brain region, it is essential to identify CRSP-1-expressing cells and to compare them with the PAM-expressing cells in the brain, pituitary and thyroid gland, in addition to the kinetic analysis for PAM in the conversion of CRSP-1-Gly into CRSP-1.

In the Northern blot analysis of CRSP-2 and CRSP-3, the band intensities of CRSP-2 and CRSP-3 mRNAs in each brain region were comparable to and about one-fifth that of CRSP-1, respectively (unpublished observation). We expected that the tissue concentration of IR-CRSP-2 and IR-CRSP-3 in the brain and thyroid gland was comparable to and about 20% that of IR-CRSP-1, respectively. However, the tissue concentrations of IR-CRSP-2 and IR-CRSP-3 in the brain, pituitary and thyroid gland are far lower than those estimated from Northern blot analysis data (Table 1). As the precursors of CRSP-2 and CRSP-3 do not possess a typical prohormone convertase cleavage site on the N-terminal side of each peptide, we surmised that the majority of IR-CRSP-2 and IR-CRSP-3 was present as their precursor forms in the cells and tissues. Therefore, tissue concentrations of IR-CRSP-2 and IR-CRSP-3 could be underestimated, because the extraction efficiency of the precursors is generally lower than those of the processed peptides.

In the present study, we isolated a new biologically active peptide from porcine brain extracts by monitoring the cAMP production in LLC-PK_1 cells, and this peptide was verified to be a glycine-extended form of CRSP-1 by the following structural analyses. Interestingly, CRSP1-Gly is equipotent as CRSP-1 and is present in all the examined tissues and brain regions along with CRSP-1 at a relatively high ratio. These facts raise the possibility that CRSP-1-Gly is not as an intermediate but an endogenous hormone and neuropeptide stimulating the CT receptor. To address this issue, more elaborate biochemical characterization, immunohistochemical and physiological analyses of CRSP-1-Gly are required to identify its physiological significance by contrasting with those of CRSP-1.

Acknowledgements

This work was supported in part by research grants from the Ministry of Education, Culture, Sports, Science and Technology (Special Coordination Funds for the Promotion of Science and Technology), from the Ministry of Health, Labor and Welfare (Cardiovascular Diseases), from the Pharmaceuticals and Medical Devices Agency (Medical Frontier Project) of Japan, and from the Protein Research Foundation (Kaneko-Narita Research Grant). The authors are grateful to Ms. A. Okabe, Y. Takada and S. Fujiwara of this institute for their technical assistance.

References

[1] Braas KM, Harakall SA, Ouafik L, Eipper BA, May V. Expression of peptidylglycine alpha-amidating monooxygenase: an in situ hybridization and immunocytochemical study. Endocrinology 1992;130:2778–88.
[2] Braas KM, Stoffers DA, Eipper BA, May V. Tissue specific expression of rat peptidylglycine alpha-amidating monooxygenase activity and mRNA. Mol Endocrinol 1989;3:1387–98.
[3] Bradbury AF, Smyth DG. Substrate specificity of an amidating enzyme in porcine pituitary. Biochem Biophys Res Commun 1983;112:372–7.
[4] Carpenter KA, Schmidt R, von Mentzer B, Haglund U, Roberts E, Walpole C. Turn structures in CGRP C-terminal analogues promote stable arrangements of key residue side chains. Biochemistry 2001;40:17–25.
[5] Cauvin A, Vandermeers-Piret MC, Vandermeers A, Coussaert E, de Neef P, Robberecht P, et al. Rat PHI, PHI-GLY and PHV (1–42) stimulate adenylate cyclase in six rat tissue and cell membranes. Peptides 1990;11:1009–14.
[6] Fahrenkrug J, Ottesen B, Palle C. Non-amidated forms of VIP (glycine-extended VIP and VIP-free acid) have full bioactivity on smooth muscle. Regul Pept 1989;26:235–9.
[7] Ferrier BM, du Vigneaud V. 9-Deamidooxytocin, an analog of the hormone containing a glycine residue in place of the glycinamide residue. J Med Chem 1966;9:55–7.
[8] Gafvelin G, Andersson M, Dimaline R, Jornvall H, Mutt V. Isolation and characterization of a variant form of vasoactive intestinal polypeptide. Peptides 1988;9:469–74.
[9] Hull RN, Cherry WR, Weaver GW. The origin and characteristics of a pig kidney cell strain, LLC-PK. In Vitro 1976;12:670–7.
[10] Katafuchi T, Hamano K, Kikumoto K, Minamino N. Identification of second and third calcitonin receptor-stimulating peptide in porcine brain. Biochem Biophys Res Commun 2003;308:445–51.
[11] Katafuchi T, Hamano K, Minamino N. Identifcation, structural determination, and biological activity of bovine and canine calcitonin receptor-stimulating peptides. Biochem Biophys Res Commun 2004;313:74–9.
[12] Katafuchi T, Kikumoto K, Hamano K, Kangawa K, Matsuo H, Minamino N. Calcitonin receptor-stimulating peptide, a new member of the calcitonin gene-related peptide family. Its isolation from porcine brain, structure, tissue distribution, and biological activity. J Biol Chem 2003;278:12046–54.
[13] Kikumoto K, Katafuchi T, Minamino N. Specificity of porcine calcitonin receptor and calcitonin receptor-like receptor in the presence of receptor-activity-modifying proteins. Hypertens Res 2003;26:S15–23.
[14] Kitamura K, Kato J, Kawamoto M, Tanaka M, Chino N, Kangawa K, et al. The intermediate form of glycine-extended adrenomedullin is the major circulating molecular form in human plasma. Biochem Biophys Res Commun 1998;244:551–5.
[15] Lin HY, Harris TL, Flannery MS, Aruffo A, Kaji EH, Gorn A, et al. Expression cloning of an adenylate cyclase-coupled calcitonin receptor. Science 1991;254:1022–4.
[16] May V, Ouafik L, Eipper BA, Braas KM. Immunocytochemical and in situ hybridization studies of peptidylglycine alpha-amidating monooxygenase in pituitary gland. Endocrinology 1990;127:358–64.

[17] McGuigan JE, Thomas HF. Physiological and immunological studies with desamidogastrin. Gastroenterology 1972;62:553–8.
[18] Olson H, Lind P, Pohl G, Henrichson C, Mutt V, Jornvall H, et al. Production of a biologically active variant form of recombinant human secretin. Peptides 1988;9:301–7.
[19] Pekary AE, Stephens R, Simard M, Pang XP, Smith V, DiStefano Jr J, et al. Release of thyrotropin and prolactin by a thyrotropin-releasing hormone (TRH) precursor, TRH-Gly: conversion to TRH is sufficient for in vivo effects. Neuroendocrinology 1990;52:618–25.
[20] Prigge ST, Kolhekar AS, Eipper BA, Mains RE, Amzel LM. Amidation of bioactive peptides: the structure of peptidylglycine alpha-hydroxylating monooxygenase. Science 1997;278:1300–5.
[21] Prigge ST, Mains RE, Eipper BA, Amzel LM. New insights into copper monooxygenases and peptide amidation: structure, mechanism and function. Cell Mol Life Sci 2000;57:1236–59.
[22] Rittel W, Maier R, Brugger M, Kamber B, Riniker B, Sieber P. Structure-activity relationship of human calcitonin. III. Biological activity of synthetic analogues with shortened or terminally modified peptide chains. Experientia 1976;32:246–8.
[23] Roberts AN, Leighton B, Todd JA, Cockburn D, Schofield PN, Sutton R, et al. Molecular and functional characterization of amylin, a peptide associated with type 2 diabetes mellitus. Proc Natl Acad Sci USA 1989;86:9662–6.
[24] Tateishi K, Arakawa F, Misumi Y, Treston AM, Vos M, Matsuoka Y. Isolation and functional expression of human pancreatic peptidylglycine alpha-amidating monooxygenase. Biochem Biophys Res Commun 1994;205:282–90.

Fusogenic Liposome can be Used as an Effective Vaccine Carrier for Peptide Vaccination to Induce Cytotoxic T Lymphocyte (CTL) Response

Toshiki SUGITA,[a,e] Tomoaki YOSHIKAWA,[a,e] Jian-Qing GAO,[a] Mariko SHIMOKAWA,[e] Atushi ODA,[a,e] Takako NIWA,[a,e] Mitsuru AKASHI,[b,e] Yasuo TSUTSUMI,[c,e] Tadanori MAYUMI,[d] and Shinsaku NAKAGAWA*,[a,e]

[a] *Department of Biopharmaceutics, Graduate School of Pharmaceutical Sciences, Osaka University; 1–6 Yamadaoka, Suita, Osaka 565–0871, Japan:* [b] *Department of Molecular Chemistry, Graduate School of Engineering, Osaka University; 2–1 Yamadaoka, Suita, Osaka 565–0871, Japan:* [c] *National Institute of Health Science, Osaka Branch Fundamental Research Laboratories for Development of Medicine; 1–1–43 Hoenzaka, Chuo-ku, Osaka 540–0006, Japan:* [d] *Department of Cell Therapeutics, Graduate School of Pharmaceutical Sciences, Kobe-Gakuin University; 518 Arise, Igawadani, Nishi-ku, Kobe 651–2180, Japan: and* [e] *CREST (Core Research for Evolutional Science and Technology) of Japan Science and Technology Corporation; Tokyo, 102–8666, Japan.*

Received August 18, 2004; accepted October 18, 2004; published online October 20, 2004

We reported previously that fusogenic liposome (FL) introduced antigen protein encapsulated in the liposome directly into the cytoplasm of the antigen presenting cells, and that it induced immune responses. In the present study, we encapsulated TAX38-46, an HTLV-I derived protein and an antigen peptide model, into FL. The ability to induce effective cytotoxic T lymphocytes (CTL) responses in immunized mice was evaluated. Results showed FL could induce CTL response effectively and suggested that FL is a potential peptide vaccine carrier.

Key words fusogenic liposome; cytotoxic T lymphocyte (CTL); peptide vaccine

Induction of cytotoxic T lymphocytes (CTL) that kill tumor cells is a critical role of immunotherapeutic agents for cancer. Most cancer vaccine strategies have focused on induction of CTL and various approaches, including DNA, virus vector or peptide vaccine, have been tested.[1)] In general, the advantages of a peptide vaccine are the induction of CTL by the epitope and the safety, stability and simplicity of peptide production. However, peptides by themselves are rather weak immunogens. Peptides usually require the addition of an adjuvant for inducing immunogenicity, and recently, incomplete Freund's adjuvant (IFA) has been widely used as a vaccine adjuvant in clinical research.[2)] However, IFA is only useful for inducing humoral immunity and thus it does not induce effective cell-mediated immune responses. In contrast, complete Freund's adjuvant (CFA) is used for CTL induction, although it cannot be applied clinically due to serious side effects, such as inflammation.[3)]

To induce cell-mediated immune responses, a peptide must be delivered through the cytoplasm to the MHC class I processing pathway. However, peptides are unable to pass through the cytoplasm alone.[4)] Therefore, we hypothesized that a vaccine carrier is required, which can deliver antigens into the cytoplasm and which exhibits adjuvant activity. We reported previously that fusogenic liposome (FL) introduces antigen protein encapsulated in the liposome directly into the cytoplasm, and that it can induce effective immune responses.[5—7)] FL is a fusion liposome in which proliferating ability is inactivated, but which retains its cell membrane fusing ability. Therefore, FL can deliver encapsulated molecules into cells. Furthermore, FL possesses immune stimulating activity.[5)] In this context, we considered FL as an ideal peptide vaccine carrier.

In the present study, we chose the TAX protein epitope (TAX 38-46; H-2D^{k-} restricted epitope in TAX, amino acid residues 38-46, sequence ARLHRHALL.[10)]), which is an immunodominant target antigen derived from the human T-cell leukemia virus type 1 (HTLV-I), as a model peptide. HTLV-I, a retro virus, is known to cause Adult T-cell leukemia (ATL).[8)] ATL is characterized by poor prognosis after chemotherapy and no effective therapy exists. Immunotherapy, which can induce strong anti HTLV-I CTL, has been proposed as an optimal approach to ATL treatment.[9)] However, an effective immunotherapeutic approach has not been developed to date.

MATERIALS AND METHODS

Cells and Animals L929 cells were cultured with RPMI-1640 containing with 10% fetal calf serum (FCS). Female C3H mice were purchased from Nippon SLC (Kyoto, Japan) and used at 6 weeks-old stage.

Fusogenic Liposome Encapsulated TAX 38-46 TAX 38-46 and FITC conjugated TAX 38-46 were purchased from SIGMA (Japan). FL was prepared as described previously.[5—7)] Briefly, lipid mixture (L-α-dimyristoyl phosphatidic acid/phosphatidylcholine/cholesterol in molar ratio of 1 : 4 : 5) was hydrated with phosphate buffered saline (PBS) or PBS containing TAX 38-46 or FITC conjugated TAX 38-46. Peptides containing liposome was prepared from these hydrated mixture by using a hand-held extruder with two layers of cellulose acetate membranes (pore size, 800 nm in diameter) (ADVANTEC, Osaka, Japan), and washed with PBS by centrifugation (20000 rpm, 40 min, 4 °C) in order to remove free peptides. These liposomes were mixed with UV-inactivated Sendai virus and incubated at 37 °C for 2 h with shaking. FL was purified by sucrose gradient centrifugation (24000 rpm, 2 h, 4 °C). The diameter of FL was detected by using ZETASIZER 3000HS (Malvern, U.K.). The concentration of peptide in FL was determined by measuring the fluorescence intensity of FITC.

^{51}Cr Release Assay For the CTL assay, TAX38-46 (50 μg), empty FL, TAX38-46 emulsified with CFA (contains 50 μg

* To whom correspondence should be addressed. e-mail: nakagawa@phs.osaka-u.ac.jp

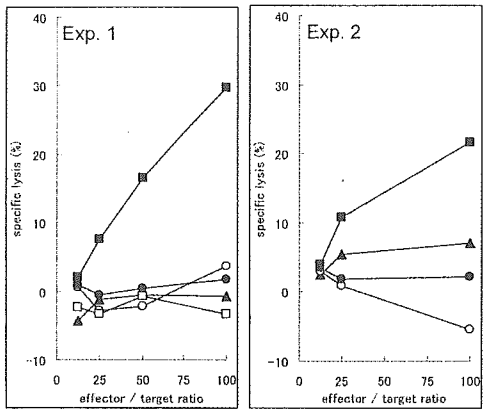

Fig. 1. TAX Peptide Encapsulated in FL Induced TAX Specific CTL

Nine days after the final immunization, mononuclear cells from the spleen of mice immunized with PBS (closed circle), TAX 38-46 alone (open circle), empty FL (open square), TAX 38-46 emulsified with CFA (closed triangle), or TAX 38-46 encapsulated in FL (closed square) were isolated and restimulated with MMC-treated TAX38-46 pulsed L929 for 5 d to enhance the frequency of antigen specific CTLs. CTL activity against TAX38-46 pulsed L929 (positive targets) or L929 (negative targets) was measured by ^{51}Cr release assay. Results were expressed as a percentage of specific lysis. Percentage of specific lysis=(percentage of positive target lysis)−(percentage of negative target lysis).

TAX38-46), or TAX38-46 encapsulated in FL (contains 30 μg TAX38-46) diluted to in total were injected into back of C3H mice (i.d.), respectively. Mice were immunized once a week for three weeks, and the spleen was harvested 9 d after the last immunization. Splenocytes were mixed with mitomycin C (MMC) treated TAX38-46 pulsed L929 for 5 d, and CTL assay was determined as follows. L929 cells (5×10^6) were pulsed with TAX 38-46 (positive targets) for 1 h at 37 °C or not (negative targets), and labeled with 200 μCi of ^{51}Cr for 2 h at 37 °C. Splenocytes were incubated with target cells (positive or negative targets) for 2 h at 37 °C. CTL activity was determined by measuring ^{51}Cr levels in the supernatants using a gamma counter. The specific lysis was determined as follows: percentage of specific lysis= (percentage of positive target lysis)−(percentage of negative target lysis).

RESULTS AND DISCUSSION

We prepared the FL encapusulating TAX 38-46. The diameter of FL was 880.1±9.5 nm. We calculated the concentrarion of peptide in FL using FITC conjugated TAX38-46. One milliliter of FL suspension at OD_{540} of 1.0 contained 29.8 μg of TAX 38-46. FL encapsulating TAX 38-46 was immunized with 100 μl at OD_{540} of 10.0.

Figure 1 demonstrates that the induction of TAX-specific CTL occurred only in response to TAX38-46-FL. CTL induction could not be detected in the TAX38-46-CFA administered group, in the TAX38-46 group, or in the empty FL group. Likewise, there was no CTL response in the group immunized with the mixture of TAX 38-46 and empty FL (data not shown). Previous reports have demonstrated that FL can deliver peptide directly into cytoplasm and that it possesses immune stimulating ability.

In a future study, we will investigate the control of peptide distribution in the cytoplasm and attempt to induce a stronger CTL response. Peptides that target the endoplasmic reticulum (ER) are able to induce stronger CTL responses because MHC class I molecules are expressed on the ER membrane.[11—13] However, because FL cannot control peptide distribution in the cytoplasm, we were unable to target the ER specifically. Therefore, the use of both FL and ER targeting sequences will more effectively induce CTL.

Acknowledgements We are grateful to Mr. M. Mori and Mr. K. Sakaguchi at NOF Corporation for supplying us with lipid mixture. This work was supported in part by "Creation of bio-devices and bio-systems with chemical and biological molecules for medical use", CREST, JST.

REFERENCES

1) Berzofsky J. A., Terabe M., Oh S., Belyakov I. M., Ahlers J. D., Janik J. E., Morris J. C., *J Clin. Invest.*, **113**, 1515—1525 (2004).
2) Romero P., Cerottini J. C., Speiser D. E., *Cancer Immunol. Immunother.*, **53**, 249—255A (2004).
3) Claassen E., de Leeuw W., de Greeve P., Hendriksen C., Boersma W., *Res. Immunol.*, **143**, 478—483 (1992)
4) Harding C. V., *Curr. Opin. Immunol.*, **3**, 3—9 (1991).
5) Hayashi A., Nakanishi T., Kunisawa J., Kondoh M., Imazu S., Tsutsumi Y., Tanaka K., Fujiwara H., Hamaoka T., Mayumi T., *Biochem. Biophys. Res. Commun.*, **261**, 824—828 (1999).
6) Nakanishi T., Hayashi A., Kunisawa J., Tsutsumi Y., Tanaka Y., Yashiro-Ohtani Y., Nakanishi M., Fujiwara H., Hamaoka T., Mayumi T., *Eur. J. Immunol.*, **30**, 1740—1747 (2000).
7) Kunisawa J., Nakanishi T., Takahashi I., Okudaira A., Tsutsumi Y., Katayama K., Nakagawa S., Kiyono H., Mayumi T., *J. Immunol.*, **167**, 1406—1412 (2001).
8) Matsuoka M., *Oncogene*, **22**, 5131—5140 (2003).
9) Hanon E., Hall S., Taylor G. P., Saito M., Davis R., Tanaka Y., Usuku K., Osamu M., Weber J. N., Bangham C. R., *Blood*, **95**, 1386—1392 (2000).
10) Lomas M., Hanon E., Tanaka Y., Bangham C. R., Gould K. G., *J. Gen. Virol.*, **83**, 641—650 (2002).
11) Minev B. R., Chavez F. L., Dudouet B. M., Mitchell M. S., *Eur. J. Immunol.*, **30**, 2115—2124 (2000).
12) Moroi Y., Mayhew M., Trcka J., Hoe M. H., Takechi Y., Hartl F. U., Rothman J. E., Houghton A. N., *Proc. Natl. Acad. Sci. U.S.A.*, **97**, 3485—3490 (2000).
13) MacAry P. M., Javid B., Floto R. A., Smith K. G., Oehlmann W., Singh M., Lehner P. J., *Immunity*, **20**, 95—106 (2004).

ARTICLE IN PRESS

Available online at www.sciencedirect.com

SCIENCE DIRECT®

ELSEVIER

Biochemical and Biophysical Research Communications 328 (2005) 1043–1050

BBRC

www.elsevier.com/locate/ybbrc

A single intratumoral injection of a fiber-mutant adenoviral vector encoding interleukin 12 induces remarkable anti-tumor and anti-metastatic activity in mice with Meth-A fibrosarcoma ☆

Jian-Qing Gao[a,b], Toshiki Sugita[a], Naoko Kanagawa[a], Keisuke Iida[a], Yusuke Eto[a], Yoshiaki Motomura[a], Hiroyuki Mizuguchi[c], Yasuo Tsutsumi[c], Takao Hayakawa[d], Tadanori Mayumi[e], Shinsaku Nakagawa[a,*]

[a] *Department of Biopharmaceutics, Graduate School of Pharmaceutical Sciences, Osaka University, 1-6 Yamadaoka, Suita, Osaka 565-0871, Japan*
[b] *Department of Pharmaceutics, College of Pharmaceutical Sciences, Zhejiang University, 353 Yan-an Road, Hangzhou, Zhejiang 310031, PR China*
[c] *National Institute of Health Sciences, Osaka Branch Fundamental Research Laboratories for Development of Medicine, 1-1-43 Hoenzaka, Chuo-ku, Osaka 540-0006, Japan*
[d] *National Institute of Health Sciences, 1-18-1 Kamiyoga, Setagaya-ku, Tokyo 158-8501, Japan*
[e] *Department of Cell Therapeutics, Graduate School of Pharmaceutical Sciences, Kobe-gakuin University, 518 Arise, Igawadani, Nishiku, Kobe 651-2180, Japan*

Received 12 January 2005

Abstract

Cytokine-encoding viral vectors are considered to be promising in cancer gene immunotherapy. Interleukin 12 (IL-12) has been used widely for anti-tumor treatment, but the administration route and tumor characteristics strongly influence therapeutic efficiency. Meth-A fibrosarcoma has been demonstrated to be insensitive to IL-12 treatment via systemic administration. In the present study, we developed an IL-12-encoding fiber-mutant adenoviral vector (AdRGD-IL-12) that showed enhanced gene transfection efficiency in Meth-A tumor cells, and the production of IL-12 p70 in the culture supernatant from transfected cells was confirmed by ELISA. In therapeutic experiments, a single low-dose (2×10^7 plaque-forming units) intratumoral injection of AdRGD-IL-12 elicited pronounced anti-tumor activity and notably prolonged the survival of Meth-A fibrosarcoma-bearing mice. Immunohistochemical staining revealed that the IL-12 vector induced the accumulation of T cells in tumor tissue. Furthermore, intratumoral administration of the vector induced an anti-metastasis effect as well as long-term specific immunity against syngeneic tumor challenge.

Keywords: Interleukin 12; Meth-A fibrosarcoma; Recombinant adenoviral vector; Anti-tumor; Anti-metastasis; Intratumoral administration; IL-12 insensitive

The immunostimulating cytokine interleukin 12 (IL-12), a heterodimeric protein composed of two disulfide-linked subunits, is secreted by dendritic cells as well as macrophages and is a key mediator of immunity [1,2]. A variety of studies have focused on the use of IL-12 in cancer therapy and, in these experiments, IL-12 has exhibited potent anti-tumor activity in a number of tumor models [3–5]. IL-12 acts on T and natural killer (NK) cells by enhancing the generation and activity of cytotoxic T lymphocytes and inducing the proliferation and production of cytokines, especially interferon-γ

☆ *Abbreviations:* Ad vector, adenoviral vector; AdRGD, RGD fiber-mutant Ad vector; FBS, fetal bovine serum; IL-12, interleukin 12; MOI, multiplicity of infection; PBS, phosphate-buffered saline; PFU, plaque-forming units; $TCID_{50}$, tissue culture infectious $dose_{50}$.

* Corresponding author. Fax: +81 6 6879 8179.
E-mail address: nakagawa@phs.osaka-u.ac.jp (S. Nakagawa).

0006-291X/$ - see front matter © 2005 Elsevier Inc. All rights reserved.
doi:10.1016/j.bbrc.2005.01.061

[6]. In addition, IL-12 inhibits tumor angiogenesis mainly through IFN-γ-dependent production of the chemokine interferon-inducible protein-10 (IP-10) [7].

Several mechanisms of the anti-tumor activity of IL-12 have been identified, and each contributes differently to the overall therapeutic outcome in a given tumor model [8–10]. Further, some tumor models, such as Meth-A and MCH-1A1 cells, are resistant to treatment with systemically administered IL-12 [11,12]. For example, intraperitoneal administration of murine recombinant IL-12 failed to inhibit the growth of Meth-A fibrosarcoma, even at a dosage of 500 ng daily for 3 days [11]. Compared with so-called IL-12-sensitive tumor cells such as OV-HM ovarian carcinoma and CSA1M fibrosarcoma, which both exhibited notable tumor regression after IL-12-stimulated T-cell infiltration into tumor tissues, Meth-A and MCH-1-A1 tumors lacked similar accumulation of immune cells [12]. Furthermore, otherwise exciting tumor regression results from preclinical studies were moderated by the severe adverse effects that occurred after systemic administration of IL-12 in murine models [13]. The clinical development of IL-12 as a single recombinant protein for systemic therapy has been tempered by pronounced toxicity and disappointing anti-tumor effects [14].

Intratumoral administration of IL-12 may offer several potential advantages over systemic dosing, such as delivery of the gene directly to the tissue of interest and avoidance of the drawbacks of systemic delivery, including the induction of toxicity, acute allergic reactions, and other adverse effects due to the encoded gene [15]. The results of one clinical trial suggest that intratumoral injection of $\leqslant 3 \times 10^{12}$ viral particles of an IL-12-encoding adenoviral vector in patients with advanced gastrointestinal malignancies is feasible and well tolerated [16].

In the present study, we constructed a recombinant adenovirus (Ad) vector that encoded IL-12 (AdRGD-IL-12); the gene transfection efficiency of AdRGD-IL-12 was higher than that of a conventional Ad vector. We also investigated the feasibility of using a single intratumoral injection of AdRGD-IL-12 to provide effective cancer treatment for primary and metastatic Meth-A fibrosarcoma. Furthermore, immunostaining was used to measure the postinjection infiltration of immune cells into tumor tissue.

Materials and methods

Cell lines and animals. Meth-A fibrosarcoma cells (BALB/c origin) were kindly provided by Dr. Hiromi Fujiwara (School of Medicine, Osaka University, Osaka, Japan) and were maintained by intraperitoneal passage in syngeneic BALB/c mice. Human embryonic kidney (HEK) 293 cells were cultured in DMEM supplemented with 10% FBS. BALB/c female mice were obtained from SLC (Hamamatsu, Japan) and used at 6–8 weeks of age. All of the experimental procedures were performed in accordance with the Osaka University guidelines for the welfare of animals in studies of experimental neoplasia.

Vector construction. The replication-deficient AdRGD vector was based on the adenovirus serotype 5 backbone with deletions of E1/E3 region. The RGD sequence for αv-integrin targeting was inserted into the HI loop of the fiber knob by using a two-step method, as previously described [17]. AdRGD-Luc, which is identical to the AdRGD-IL-12 vectors but with the substitution of the luciferase gene expression cassette for the cytokine, was used as negative control vector in the present study. The replication-deficient AdRGD-IL-12, which carries the murine IL-12 gene derived from mIL-12 BIA/pBluescript II KS(−) [18] (kindly provided by Prof. Hiroshi Yamamoto, Graduate School of Pharmaceutical Sciences, Osaka University, Suita, Japan), was constructed by an improved in vitro ligation method using pAdHM15-RGD [19,20]. The expression cassette, which was designed to be transcribed in order from the IL-12 p35 cDNA through the internal ribosome entry site sequence to the IL-12 p40 cDNA under the control of the cytomegalovirus promoter, was inserted into the E1-deletion region of the E1/E3-deleted Ad vector (Fig. 1). All vectors were propagated in HEK293 cells, purified by two rounds of CsCl gradient centrifugation, dialyzed with phosphate-buffered saline (PBS) containing 10% glycerol, and stored at −80 °C. The number of viral particles in vector stock was determined spectrophotometrically by the method of Maizel et al. [21]. Titers (tissue culture infectious dose$_{50}$; TCID$_{50}$) of infective AdRGD particles were evaluated by the end-point dilution method using HEK293 cells and expressed as plaque-forming units (PFU).

Gene expression by AdRGD-Luc or conventional Ad-Luc in Meth-A cells. Meth-A cells were plated in 96-well plates at a density of 2×10^3 cells/well and incubated with Ad-Luc or AdRGD-Luc at concentrations of 1250, 2500, 5000, or 10,000 viral particles/cell for 1.5 h. Cells were then washed with PBS and cultured for an additional 48 h. Subsequently, the cells were washed, collected, and lysed with Luciferase Cell Culture Lysis buffer (Promega, USA), and their luciferase activity was measured by the Luciferase Assay System (Promega,

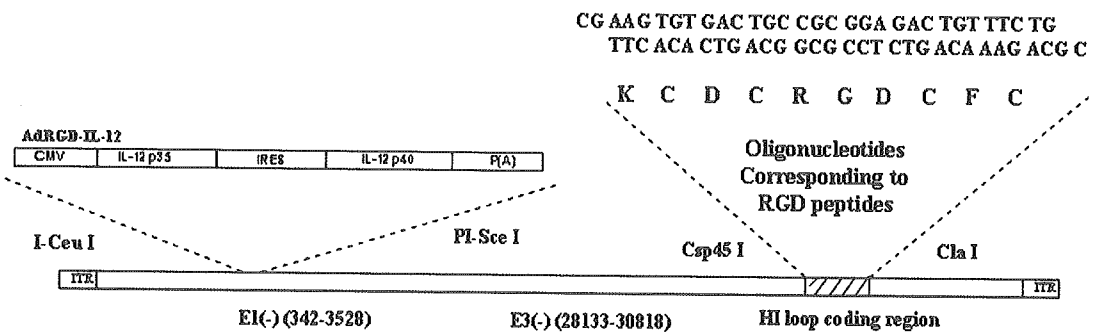

Fig. 1. Construction of IL-12 encoding fiber-mutant adenoviral vector.

USA) and Microlumat Plus LB96 (Perkin-Elmer) according to the manufacturer's instructions.

Analysis of gene transduction of AdRGD-IL-12 in vitro. Meth-A cells were plated in six-well plates at a density of 5×10^5 cells/well and transfected with AdRGD-IL-12 for 24 h at various multiplicities of infection (MOIs) in 2 ml RPMI 1640 medium containing 10% FBS. After three washes of the transfected cells with PBS, a 1.5-ml aliquot of culture medium was added to each well. The supernatants were collected after 24 h, and the amount of IL-12 p70 in each sample was measured with a murine IL-12 p70 ELISA kit (Biosource International, Camarillo, CA, USA) according to the manufacturer's instructions.

Tumor inoculation and intratumoral administration of vectors in animal experiments. Meth-A cells were inoculated intradermally into the flanks of BALB/c mice at 2×10^6 cells/mouse. After 7 days, established tumors (diameter, 9–10 mm) were injected with each vector at 2×10^7 plaque-forming units (PFU) in 50 μl PBS. Tumor size (length and width in mm) was measured twice weekly; animals were euthanized when either of the two parameters exceeded 20 mm. At 3 months after complete regression of the primary tumors, mice were challenged with freshly isolated Meth-A tumor cells or CT26 cells by intradermal injection of 1×10^6 cells into the flank.

Immunohistochemical staining. T-cell infiltration into the Meth-A tumors after intratumoral injection of AdRGD-IL-12 was determined by immunohistochemical analysis. Tumor-bearing mice were euthanized 6 days after administration of AdRGD-IL-12 or the control vector. The tumor nodules were harvested, embedded in OCT compound (Sakura, Torrance, CA, USA), and stored at −80 °C. Frozen thin (6-μm) sections of the nodules were fixed in 4% paraformaldehyde solution, washed with Tris-buffered saline (TBS), and incubated in methanol containing 0.3% hydrogen peroxide for 30 min at room temperature to block endogenous peroxidase activity. The sections were incubated with the optimal dilution of the primary antibody—either rabbit anti-human CD3 antibody (DakoCytomation) or normal rabbit IgG (Santa Cruz Biotechnology)—for 60 min at room temperature. Bound primary antibody was detected after incubation with the secondary antibody from the EnVision+ System (DakoCytomation) for 30 min, followed by a 15-min wash in TBS. The sections were stained with DAB (DakoCytomation) and finally counterstained with hematoxylin (DakoCytomation). We randomly selected six fields from different tumor sections and counted the immunostained cells under a light microscope at 400× magnification.

Experiments on metastatic tumor. We intradermally inoculated mice with 2×10^6 Meth-A cells as described earlier and, 5 days later, injected 8×10^4 cells intravenously. Two days after the intravenous injection, intratumoral injection of AdRGD-IL-12 (2×10^7 PFU) was carried out. The size of the primary tumor was measured twice weekly, and the lungs were harvested 2 weeks after the intravenous injection. The lungs were weighed, sectioned for histology, and stained with hematoxylin and eosin. Metastases in the lungs were identified under a light microscope.

Statistical analysis. Student's t test was used for statistical comparison when applicable. Differences were considered statistically significant at $P < 0.05$.

Results

Meth-A tumor cells transfected with the fiber-mutant adenoviral vector induce higher luciferase gene expression than do those induced with the conventional vector

To evaluate the gene transfection efficiency of the fiber-mutant Ad vector developed for this study, Meth-A cells were transfected with either the conventional Ad-Luc vector or the fiber-mutant AdRGD-Luc vector at various MOIs and the luciferase activity was measured. The luciferase gene expression due to transfection of the fiber-mutant vector was much higher than that from the conventional vector (Fig. 2). For example, at 5000 and 10,000 viral particles/cell, 16.8-fold and 15.7-fold greater gene expression, respectively, was obtained in response to AdRGD-Luc than to Ad-Luc. These results show that insertion of the RGD peptide into the viral fiber enhanced the transfection efficiency of the Ad vector into Meth-A cells.

Expression of IL-12 p70 in Meth-A cells via transfection of AdRGD-IL-12

The IL-12-encoding fiber-mutant adenoviral vector AdRGD-IL-12 was developed as shown in Fig. 1. To confirm the biological activity of AdRGD-IL-12, we used an ELISA to measure the amount of IL-12 in the

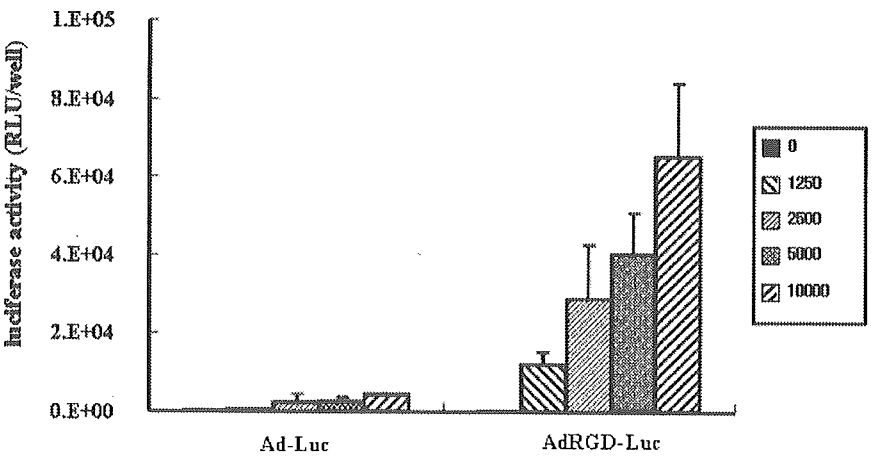

Fig. 2. Gene expression by AdRGD-Luc or conventional Ad-Luc in Meth-A cells. Meth-A cells (2×10^3/well) in 96-well plates were treated with Ad-Luc or AdRGD-Luc at the indicated numbers of viral particles/cell for 1.5 h. Cells were washed and cultured for an additional 48 h. Subsequently, the cells were washed, collected, and their luciferase activity was measured. Data are presented as means ± SE of relative light units (RLUs)/well from three experiments.

supernatants of transfectants. Meth-A cells transfected with AdRGD-IL-12 showed dose-dependent concentrations of IL-12 p70 in the supernatants. In contrast, no detectable IL-12 p70 was present in the culture media of cells that had not been transfected (Fig. 3).

Anti-tumor activity and long-term specific immune response are induced by intratumoral injection of AdRGD-IL-12

The growth of Meth-A tumors was suppressed dramatically, and complete regression occurred in about 70% of the tumor-bearing mice after a single intratumoral injection of 2×10^7 PFU of AdRGD-IL-12. In contrast, the AdRGD-Luc group showed no apparent anti-tumor effect (Fig. 4A). In addition, the relative survival rates further demonstrated prolonged survival after treatment with IL-12 (Fig. 4B). In the rechallenge experiment, mice showing complete regression were reinoculated intradermally with Meth-A or CT26 cells 90 days after the initial injection of tumor cells. All of the mice challenged with Meth-A cells remained tumor-free for at least 2 months (Table 1). In contrast, 100% of the mice challenged with CT26 developed palpable tumors within 2 weeks. These results indicate the generation of specific immunity against Meth-A tumor cells in those mice that rejected Meth-A upon treatment with IL-12.

Intratumoral administration of AdRGD-IL-12 induces the infiltration of T cells into Meth-A tumors

To investigate the anti-tumor mechanism of AdRGD-IL-12, tumor tissues were subjected to immunohistochemical staining for CD3 six days after treatment with AdRGD-IL-12 or AdRGD-Luc. Tissues from mice that received AdRGD-IL-12 demonstrated significantly increased accumulation of $CD3^+$ T cells compared
with animals injected with either AdRGD-Luc or PBS (Fig. 5).

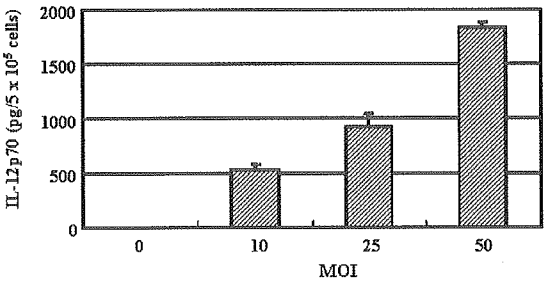

Fig. 3. Production of IL-12 p70 from Meth-A cells transfected with AdRGD-IL-12. We transfected 5×10^5 Meth-A cells with AdRGD-IL-12 for 24 h at the indicated multiplicities of infection (MOIs). Then the cells were cultured for a further 24 h with fresh medium. The supernatants were collected and the IL-12 p70 level was measured by ELISA.

Table 1
Specific long-term anti-tumor immune response to IL-12 treatment

Groups	Challenging cell	Tumor rejected mice/challenged mice
Intact mice	Meth-A[a]	0/5
Meth-A rejected[c]	Meth-A[a]	5/5
Meth-A rejected[d]	CT26[b]	0/3

[a] Challenged with 1×10^6 cells.
[b] Challenged with 3×10^5 cells.
[c] Meth-A cured; Meth-A rechallenged.
[d] Meth-A cured; CT26 rechallenged.

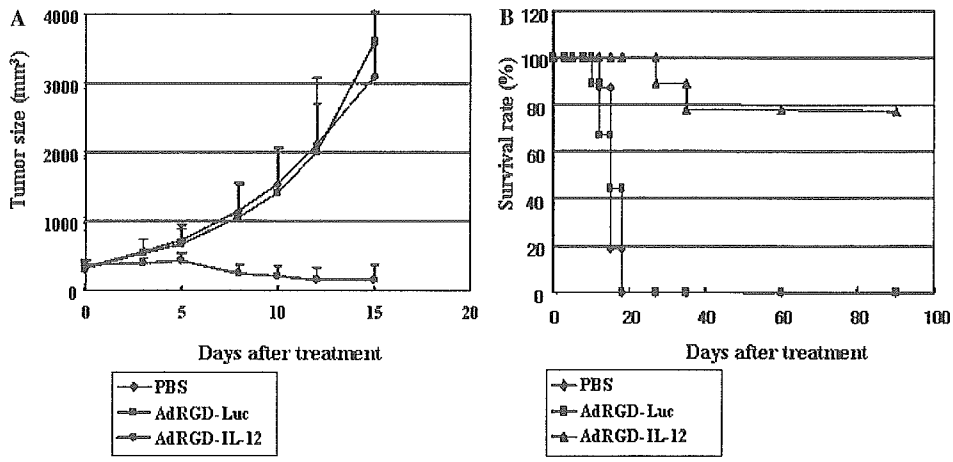

Fig. 4. Growth in BALB/c mice of established Meth-A tumor cells injected intratumorally with IL-12-encoding adenoviral vector. Mice were inoculated intradermally in the flank with 2×10^6 Meth-A cells (100 μl in RPMI 1640). They were then intratumorally injected with 2×10^7 PFU AdRGD-IL-12, AdRGD-Luc, or PBS. Tumor volume was calculated after measuring the length and width of tumors at the indicated time points, and data are expressed as means ± SE of results obtained from at least eight mice. Animals were euthanized when either the length or width of the tumor exceeded 20 mm. (A) Average tumor size. (B) Survival rate (%) of mice.

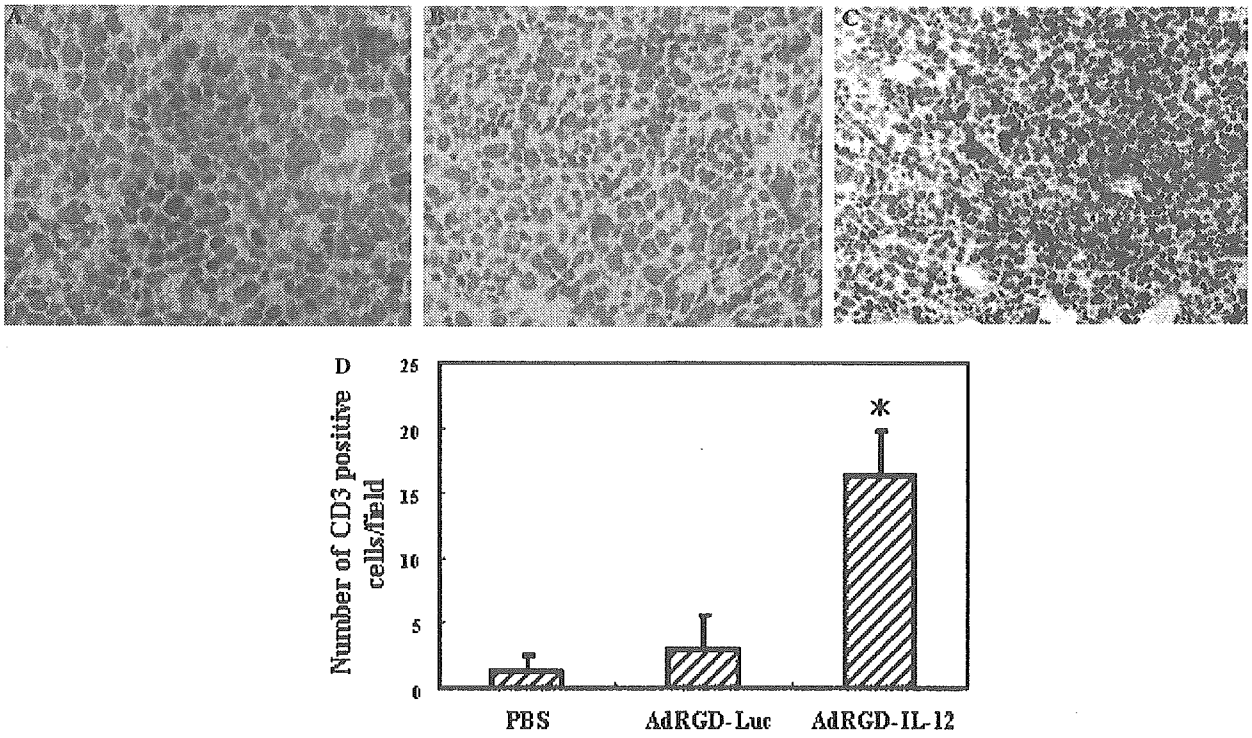

Fig. 5. Intratumoral injection of AdRGD-IL-12 induced the infiltration of $CD3^+$ T cells into Meth-A tumors. Representative views of tumor nodules from mice, harvested 6 days after intratumoral injection of the indicated vectors and controls, and stained for CD3. (A) PBS, (B) AdRGD-Luc, (C) AdRGD-IL-12. The photographs were obtained under light microscopy at 400× magnification. (D) Six fields from different tumor sections were randomly selected and positive cell number infiltrated into tumor tissue was counted. $^*P < 0.05$ with Student's t test in groups between treated with AdRGD-IL-12 and AdRGD-Luc or PBS.

A

Group	Metastasis-free mice/mice in group	Occurrence of Metastasis (%)
PBS	0/8	100%
AdRGD-Luc	1/9	89%
AdRGD-IL-12	8/9	11%

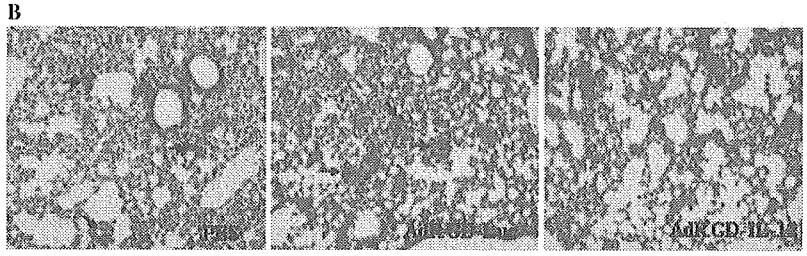

Fig. 6. Anti-metastatic activity due to intratumoral injection of AdRGD-IL-12 into Meth-A fibrosarcoma. (A) Incidence of metastasis in each group. (B) Photomicrographs of lung tissue harvested 2 weeks after treatment and stained with hematoxylin and eosin. The photographs were obtained under light microscopy at 10× magnification. The arrows indicate micrometastasizing tumor.

Anti-metastatic activity is induced by intratumoral injection of AdRGD-IL-12

We then sought to evaluate whether intratumoral injection of AdRGD-IL-12 would induce anti-tumor effects against both the primary and metastatic tumors. Our results showed that single intratumoral injection of AdRGD-IL-12 induced pronounced anti-metastasis activity (Figs. 6A and B) while maintaining tumor-suppressive activity toward the primary tumor, similar to

that shown in Fig. 4 (data not shown). Compared with the control group treated with AdRGD-Luc, in which about 90% of the mice had readily discernable lung metastasis, only one of nine animals treated with AdRGD-IL-12 demonstrated metastasis.

Discussion

Viral vector-encoded chemokines and cytokines are used widely in cancer gene therapy [22,23]. IL-12 has demonstrated remarkable anti-tumor activity when used directly as a recombinant protein or after various viral and non-viral vectors have been used to transfer its genes [24–26]. The development of an efficient vector is pivotal for gene therapy. Because of its high transfection efficiency and because it can transfect both dividing and quiescent cells, Ad vectors are used widely in gene therapy protocols: about 26% of gene therapy clinical trials use Ad vectors as gene carriers [27,28]. However, the lack of Coxsackie adenovirus receptor (CAR), which is an important receptor for conventional Ad vector infection, in many types of malignant cells impairs the tranfection efficiency with Ad vector [29]. Meth-A fibrosarcoma has been confirmed by RT-PCR to be deficient in expression of CAR but with expression of integrin (data not shown). Our previous reports have also shown that insertion of the RGD peptide into the fiber sequences of Ad vectors induces enhanced gene transfection in CT26 and A2058 cells [30,31]. The results of our present study also demonstrate that the fiber-mutant Ad vector induced enhanced expression of the encoded luciferase gene in Meth-A fibrosarcoma cells compared with the expression due to conventional vector (Fig. 2). Furthermore, we confirmed the presence of IL-12 p70 in the supernatant of Meth-A cells transfected with AdRGD-IL-12 (Fig. 3).

Systemic administration of recombinant IL-12 at high doses induces adverse effects associated with high systemic peak concentrations [32,33]. Therefore, gene transfer methods are designed to confine IL-12 production to the tumor environment, thereby preventing systemic toxicity. Tumor cells, dendritic cells, and autologous fibroblasts have been transfected with recombinant adenoviruses or retroviruses to secrete IL-12 locally and have shown favorable efficacy and safety profiles [34,35]. Several groups have shown that intratumoral injection of an Ad vector encoding IL-12 efficiently eradicates experimental gastrointestinal cancer [36,37]. Disadvantages of direct topical administration include tissue damage, and some tumor sites may be inaccessible even to computed tomography-guided percutaneous injection and radiographically directed delivery [38]. However, these limitations favor those types of gene therapy that do not require all tumor cells or tumor masses that express the gene.

Meth-A has shown that it is an IL-12-insensitive tumor cell, in that established tumors could not be treated efficiently via systemic administration of IL-12 and could not even be suppressed effectively (i.e., only 42.5% of mice rejected the tumor) after transfection of an IL-12-containing retroviral vector [12,39]. In our present study, however, a single intratumoral injection of a relatively low dose of AdRGD-IL-12 (2×10^7 PFU) elicited strong anti-tumor activity against established tumors (i.e., diameter of about 10 mm at the beginning of treatment; Fig. 4A). Treatment induced complete tumor regression in about 70% of tumor-bearing mice, and the growth rates of the remaining tumors seem to have been retarded (individual data not shown). Treatment also prolonged the survival of the mice significantly compared with that of the group injected with AdRGD-Luc, a control vector (Fig. 4B). Meanwhile, no detectable IL-12 and IFN-γ existed in the sera after treatment (data not shown)—findings that are consistent with those other reports [40]. Furthermore, intratumoral injection of AdRGD-IL-12 induced a profound long-term specific anti-tumor immunity in mice with complete regression of the initial Meth-A lesion (Table 1).

Studies have shown that IL-12 elicits tumor regression after induction of T-cell migration to tumor sites [41]. The failure of IL-12 therapy in Meth-A via systemic administration is thought to be due to the inability to recruit immune cell migration into tumor cells, and further investigation has indicated a key role of the peritumoral stroma/stromal vasculature in the acceptance of the tumor-infiltrating T cells that are a prerequisite for IL-12-induced tumor regression [12]. Our results similarly demonstrated the accumulation and uniform distribution of $CD3^+$ T cells in the tumor after intratumoral injection, thus supporting the notion that the pronounced anti-tumor effect is related to immune cell infiltration (Fig. 5). However, it remains unclear why intratumoral injection but not systemic administration induces immune cell accumulation in tumor tissue.

We also evaluated the anti-metastasis activity associated with a single intratumoral injection of AdRGD-IL-12. Metastasis is a challenge for cancer treatment, especially because almost all immunotherapy performed in the clinical setting is adjuvant treatment given after surgical reduction of the primary tumor mass for controlling recurrence and metastasis. Interestingly, the single intratumoral injection of AdRGD-IL-12 did induce anti-tumor activity toward disseminated tumors in the lung: histopathology confirmed the complete absence of metastatic tumors in eight of the nine mice tested (and only sporadic residual tumor in the remaining animal). In contrast, all mice that received intratumoral injection of the control vector developed metastases, suggesting that local expression of IL-12 also stimulates the systemic immune response to subsequently affect distant malignant cells.

All the results of our present study indicate that a single intratumoral injection of an IL-12-encoding fiber-mutant Ad vector induces T-cell infiltration into stroma-deficient Meth-A fibrosarcoma and is effective in the treatment of, and protection against challenge with, syngeneic tumors. Our results also suggest that a single intratumoral administration of AdRGD-IL-12 can induce a curative immune response in the face of a micrometastasizing tumor.

Acknowledgments

This study was supported by grants from the Ministry of Health, Labor, and Welfare of Japan and by Grants-in-Aid for Scientific Research on Priority Areas from the Ministry of Education, Culture, Sports, Science and Technology of Japan.

References

[1] M.J. Brunda, Interleukin-12, J. Leukoc. Biol. 55 (1994) 280–288.
[2] G. Trinchieri, Interleukin-12: A proinflammatory cytokine with immunoregulatory functions that bridge innate resistance and antigen-specific adaptive immunity, Annu. Rev. Immunol. 13 (1995) 251–276.
[3] M.P. Colombo, G. Trinchieri, Interleukin-12 in anti-tumor immunity and immunotherapy, Cytokine Growth Factor Rev. 13 (2002) 155–168.
[4] A. Maheshwari, S. Han, R.I. Mahato, S.W. Kim, Biodegradable polymer-based interleukin-12 gene delivery: Role of induced cytokines, tumor infiltrating cells and nitric oxide in anti-tumor activity, Gene Ther. 9 (2002) 1075–1084.
[5] J.W. Yockman, A. Maheshwari, S.O. Han, S.W. Kim, Tumor regression by repeated intratumoral delivery of water soluble lipopolymers/p2CMVmIL-12 complexes, J. Control Release 87 (2003) 177–186.
[6] C.L. Nastala, H.D. Edington, T.G. McKinney, H. Tahara, M.A. Nalesnik, M.J. Brunda, M.K. Gately, S.F. Wolf, R.D. Schreiber, W.J. Storkus, Recombinant IL-12 administration induces tumor regression in association with IFN-γ production, J. Immunol. 153 (1994) 1697–1706.
[7] W.G. Yu, M. Ogawa, J. Mu, K. Umehara, T. Tsujimura, H. Fujiwara, T. Hamaoka, IL-12-induced tumor regression correlates with in situ activity of IFN-gamma produced by tumor-infiltrating cells and its secondary induction of anti-tumor pathways, J. Leukoc. Biol. 62 (1997) 450–457.
[8] J. Cui, T. Shin, T. Kawano, H. Sato, E. Kondo, I. Toura, Y. Kaneko, H. Koseki, M. Kanno, M. Taniguchi, Requirement for valpha 14 NKT cells in IL-12-mediated rejection of tumors, Science 278 (1997) 1623–1626.
[9] M. Iwasaki, W.G. Yu, Y. Uekusa, C. Nakajima, Y.F. Yang, P. Gao, R. Wijesuriya, H. Fujiwara, T. Hamaoka, Differential IL-12 responsiveness of T cells but not of NK cells from tumor-bearing mice in IL-12-responsive versus -unresponsive tumor models, Int. Immunol. 12 (2000) 701–709.
[10] M.J. Smyth, M. Taniguchi, S.E. Street, The anti-tumor activity of IL-12: Mechanisms of innate immunity that are model and dose dependent, J. Immunol. 165 (2000) 2665–2670.
[11] H. Fujiwara, T. Hamaoka, Antitumor and antimetastatic effects of interleukin 12, Cancer Chemother. Pharmacol. 38 (1996) S22–S26.
[12] M. Ogawa, K. Umehara, W.G. Yu, Y. Uekusa, C. Nakajima, T. Tsujimura, T. Kubo, H. Fujiwara, T. Hamaoka, A critical role for a peritumoral stromal reaction in the induction of T-cell migration responsible for interleukin-12-induced tumor regression, Cancer Res. 59 (1999) 1531–1538.
[13] M.J. Brunda, L. Luistro, R.R. Warrier, R.B. Wright, B.R. Hubbard, M. Murphy, S.F. Wolf, M.K. Gately, Antitumor and antimetastasis activity of interleukin 12 against murine tumors, J. Exp. Med. 178 (1993) 1223–1230.
[14] J. Cohen, IL-12 deaths: Explanation and a puzzle, Science 270 (1995) 908.
[15] E.T. Akporiaye, E. Hersh, Clinical aspects of intratumoral gene therapy, Curr. Opin. Mol. Ther. 1 (1999) 443–453.
[16] B. Sangro, G. Mazzolini, J. Ruiz, M. Herraiz, J. Quiroga, I. Herrero, A. Benito, J. Larrache, J. Pueyo, J.C. Subtil, C. Olague, J. Sola, B. Sadaba, C. Lacasa, I. Melero, C. Qian, J. Prieto, Phase I trial of intratumoral injection of an adenovirus encoding interleukin-12 for advanced digestive tumors, J. Clin. Oncol. 22 (2004) 1389–1397.
[17] H. Mizuguchi, N. Koizumi, T. Hosono, N. Utoguchi, Y. Watanabe, M.A. Kay, T. Hayakawa, A simplified system for constructing recombinant adenoviral vectors containing heterologous peptides in the HI loop of their fiber knob, Gene Ther. 8 (2001) 730–735.
[18] S. Obana, H. Miyazawa, E. Hara, T. Tamura, H. Nariuchi, M. Takata, S. Fujimoto, H. Yamamoto, Induction of anti-tumor immunity by mouse tumor cells transfected with mouse interleukin-12 gene, Jpn. J. Med. Sci. Biol. 48 (1995) 221–236.
[19] H. Mizuguchi, M.A. Kay, Efficient construction of a recombinant adenovirus vector by an improved in vitro ligation method, Hum. Gene Ther. 9 (1998) 2577–2583.
[20] H. Mizuguchi, M.A. Kay, A simple method for constructing E1- and E1/E4-deleted recombinant adenoviral vectors, Hum. Gene Ther. 10 (1999) 2013–2017.
[21] J.V. Maizel Jr., D.O. White, M.D. Scharff, The polypeptides of adenovirus. I. Evidence for multiple protein components in the virion and a comparison of types 2, 7A, and 12, Virology 36 (1968) 115–125.
[22] J.Q. Gao, Y. Tsuda, K. Katayama, T. Nakayama, Y. Hatanaka, Y. Tani, H. Mizuguchi, T. Hayakawa, O. Yoshie, Y. Tsutsumi, T. Mayumi, S. Nakagawa, Anti-tumor effect by interleukin-11 receptor alpha-locus chemokine/CCL27, introduced into tumor cells through a recombinant adenovirus vector, Cancer Res. 63 (2003) 4420–4425.
[23] R. Dummer, J.C. Hassel, F. Fellenberg, S. Eichmuller, T. Maier, P. Slod, B. Acres, P. Bleuzen, V. Bataille, P. Squiban, G. Burg, M. Urosevic, Adenovirus-mediated intralesional interferon-gamma gene transfer induces tumor regressions in cutaneous lymphomas, Blood 104 (2004) 1631–1638.
[24] A.M. Orengo, E.D. Carlo, A. Comes, M. Fabbi, T. Piazza, M. Cilli, P. Musiani, S. Ferrini, Tumor cells engineered with IL-12 and IL-15 genes induce protective antibody responses in nude mice, J. Immunol. 171 (2003) 569–575.
[25] S. Zheng, G. Zeng, D.S. Wilkes, G.E. Reed, R.C. McGarry, J.N. Eble, L. Cheng, Dendritic cells transfected with interleukin-12 and pulsed with tumor extract inhibit growth of murine prostatic carcinoma in vivo, Prostate 55 (2003) 292–298.
[26] S. Gyorffy, K. Palmer, T.J. Podor, M. Hitt, J. Gauldie, Combined treatment of a murine breast cancer model with type 5 adenovirus vectors expressing murine angiostatin and IL-12: A role for combined anti-angiogenesis and immunotherapy, J. Immunol. 166 (2001) 6212–6217.
[27] Wiley website: <http://www.wiley.co.uk/genmed/clinical>.
[28] J.A. St. George, Gene therapy progress and prospects: Adenoviral vectors, Gene Ther. 10 (2003) 1135–1141.
[29] H. Wu, T. Han, J.T. Lam, C.A. Leath, I. Dmitriev, E. Kashentseva, M.N. Barnes, R.D. Alvarez, D.T. Curiel, Preclinical evalu-